Vlnovody s velkým kontrastem indexu lomu

„Fotonický drát“

(vlnovod s velkým kontrastem indexu lomu)

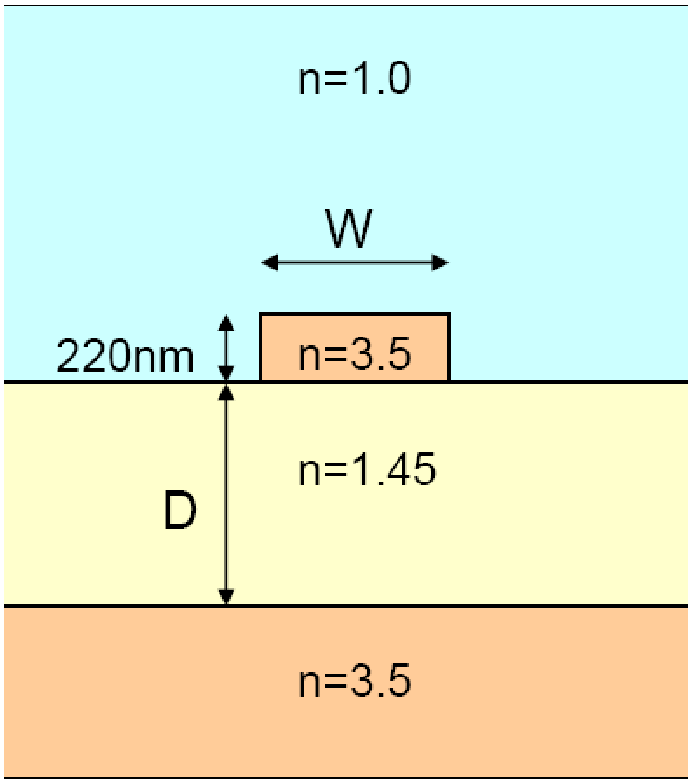

Rozložení elektromagnetického pole základního vidu TE_{00}

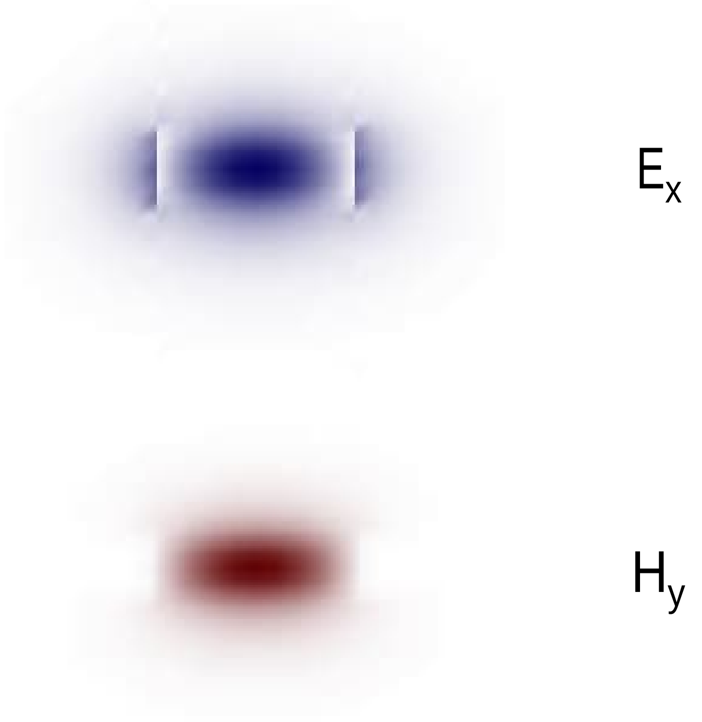

Vazba do „nanofotonických“ vlnovodů

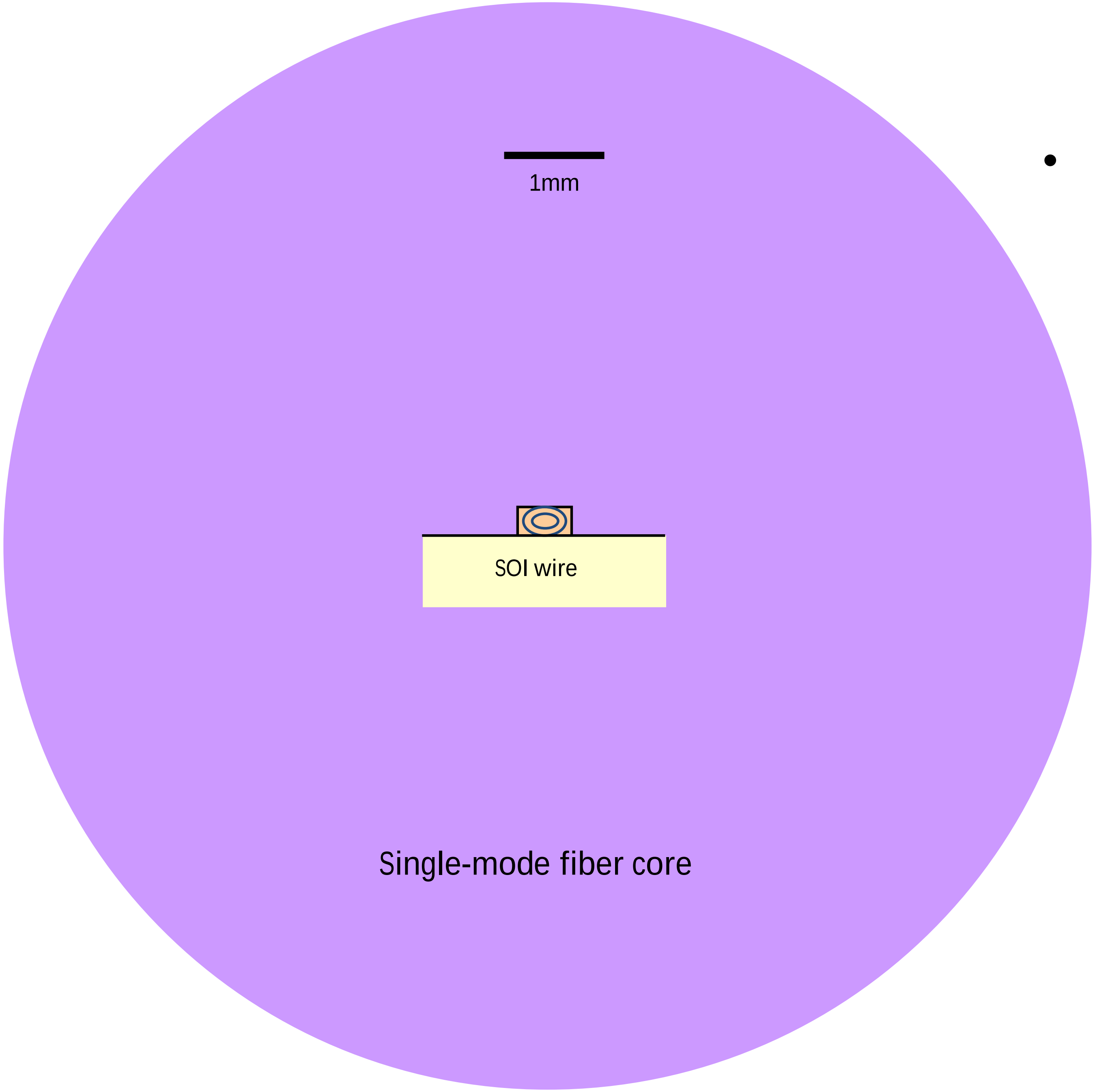

- Problémy:
  - Účinná vazba mezi submikrometrovým vlnovodem a vláknem
  - Je nutný konvertor velikosti vidového pole:
    - v horizontální rovině
    - ve vertikální rovině (obtížnější)
  - Polarizační problém

„Adiabatický přechod“ mezi vlnovody velmi různých profilů / kontrastů

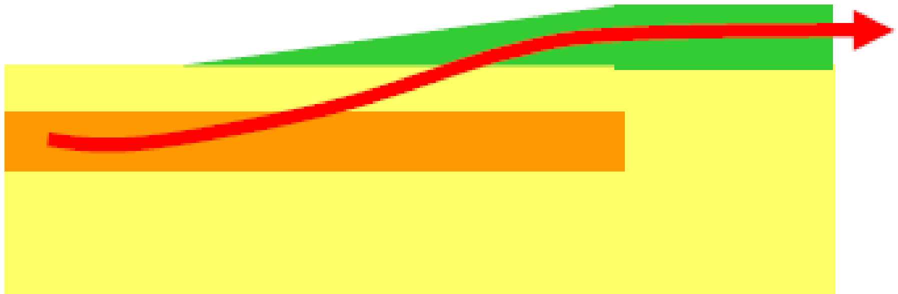

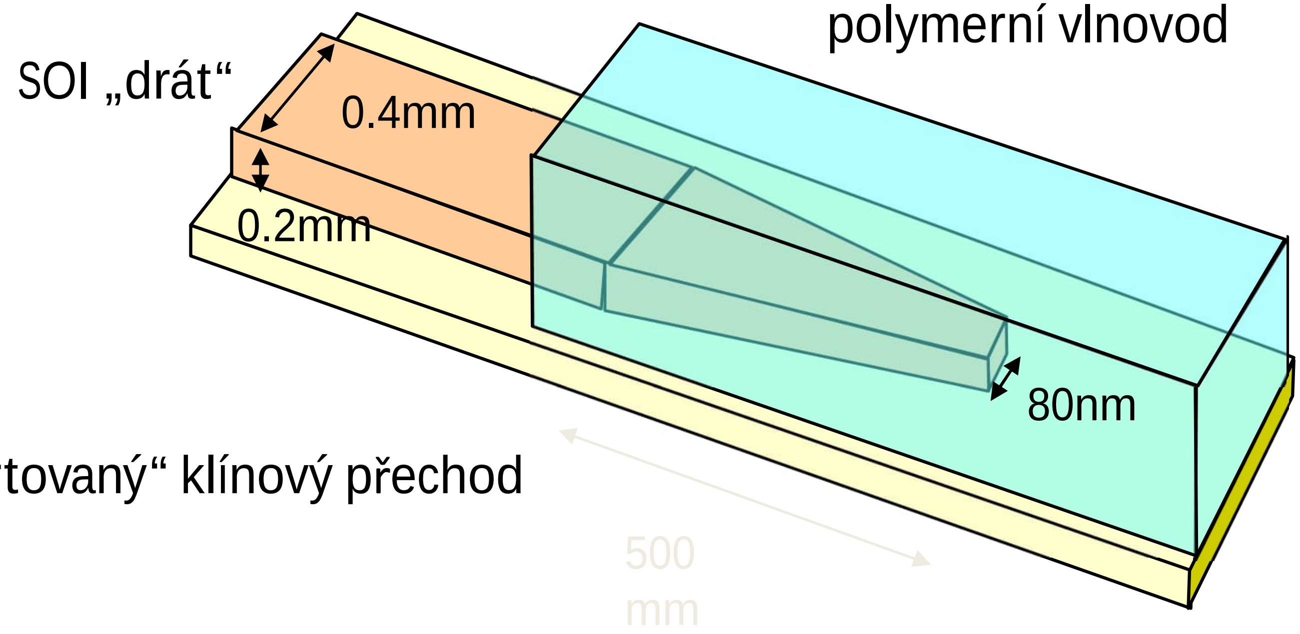

Křemíkové vlnovody se subvlnovými strukturami (subwavelength grating waveguide, SWG)

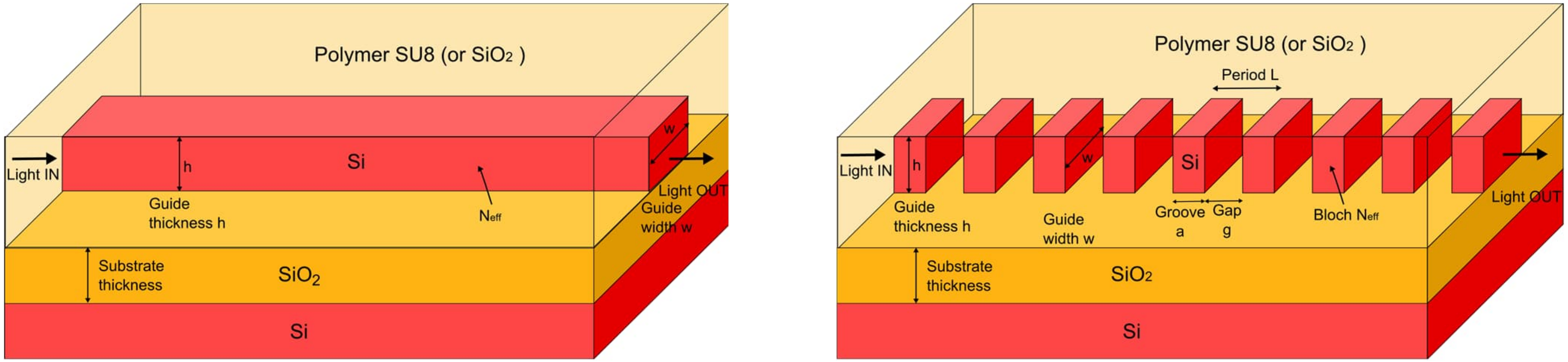

Schematic picture of (a) a strip channel waveguide and (b) SWG waveguide considered in this contribution. In both cases, Si guide (either continuous or segmented) on SiO_2 substrate, embedded in SU8 polymer (or, alternatively in SiO_2 cladding) are considered; h represents the guide thickness, w guide width, L is the SWG period (with Si groove dimension a, and gap g).

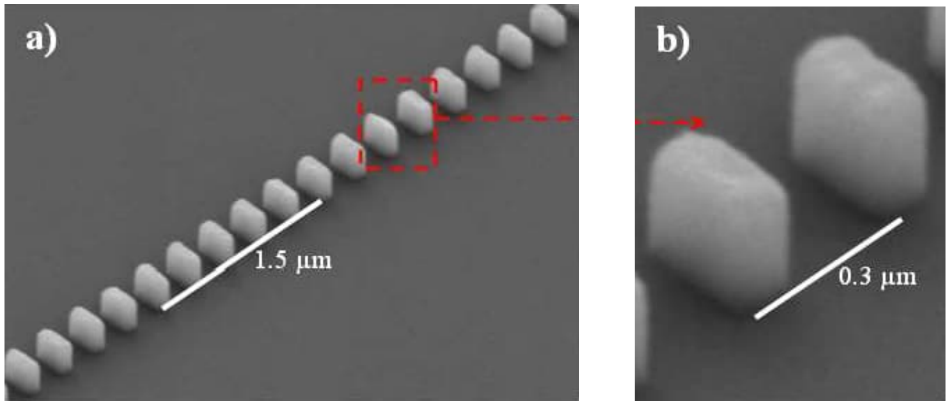

Scanning electron microscope (SEM) images of fabricated structures including: a) SWG straight waveguide with Λ = 300 nm, w = 250 nm and a duty cycle of 33%. b) Detail of two SWG segments.

P. J. Bock, Optics Express, 18(19), 20251 (2010).

- SWG waveguide - a new type of microphotonic waveguide
- Practical implementations to fiber-chip coupling, waveguide crossing and refractive index engineering

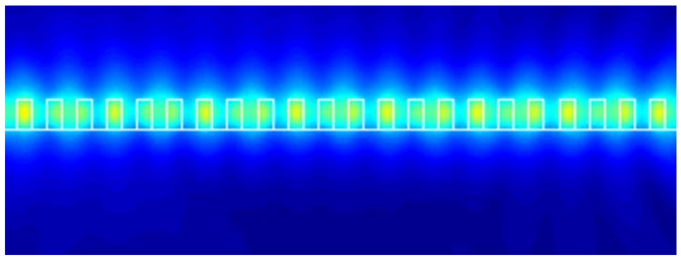

ELEMENTÁRNÍ TEORIE EFEKTIVNÍHO PROSTŘEDÍ (Effective medium theory, EMT)

Vrstevnaté prostředí s parametry $\varepsilon_1,\ d_1$ a $\varepsilon_2,\ d_2$

$d_1,\ d_2 \ll \lambda$

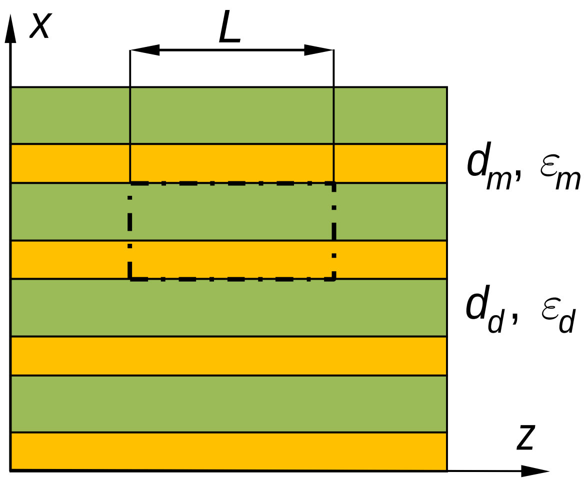

Ekvivalentní kapacitor s deskami podél x:

$$C_{eq} = \frac{\varepsilon_1 d_1}{L} + \frac{\varepsilon_2 d_2}{L} = \frac{\varepsilon_\parallel (d_1 + d_2)}{L};$$

$\varepsilon_\parallel$ ...eff. permittivita

Tedy $\varepsilon_\parallel = f\varepsilon_1 + (1-f)\varepsilon_2,$ $\quad f = \dfrac{d_1}{d_1 + d_2} = \dfrac{d_1}{L}$

Ekvivalentní kapacitor s deskami podél z: $0 \le f \le 1.$

$$\frac{1}{C_{eq}} = \frac{d_1}{\varepsilon_1 L} + \frac{d_2}{\varepsilon_2 L} = \frac{(d_1 + d_2)}{\varepsilon_\perp L}$$

$\varepsilon_\perp$ ...eff. permittivita,

Tedy $\dfrac{1}{\varepsilon_\perp} = \dfrac{1}{\varepsilon_1} f + \dfrac{1}{\varepsilon_2}(1-f),$ $\quad \varepsilon_\perp = \dfrac{\varepsilon_1 \varepsilon_2}{f\varepsilon_2 + (1-f)\varepsilon_1},$

Efektivní prostředí je anizotropní, jednoosé, s tenzorem permitivity

$$\boldsymbol{\varepsilon}_{eff} = \begin{pmatrix} \varepsilon_\perp & 0 & 0 \\ 0 & \varepsilon_\parallel & 0 \\ 0 & 0 & \varepsilon_\parallel \end{pmatrix}$$

J. C. Maxwell Garnett, "Colours in metal glasses and in metallic films,"
Philosophical Transaction of the Royal Society London 203, 385-420 (1904).

Složitější subvlnové vlnovodné struktury

Vazební člen - vidový transformátor

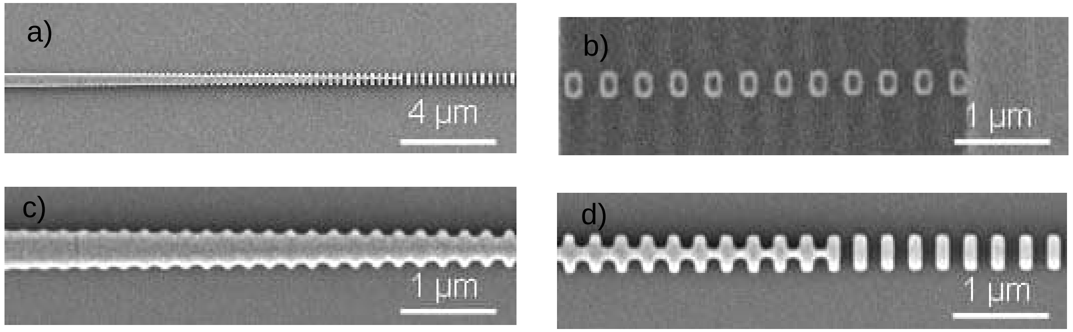

Subwavelength grating mode transformer.
a) SEM image of the coupler,
b) low - confinement section near the chip edge,
c) high-confinement section near the strip waveguide,
d) Intermediate section.

P. J. Bock et al., 7th IEEE Conference on Group IV Photonics, Sept. 2010, Beijing

Křížení segmentovaných vlnovodů

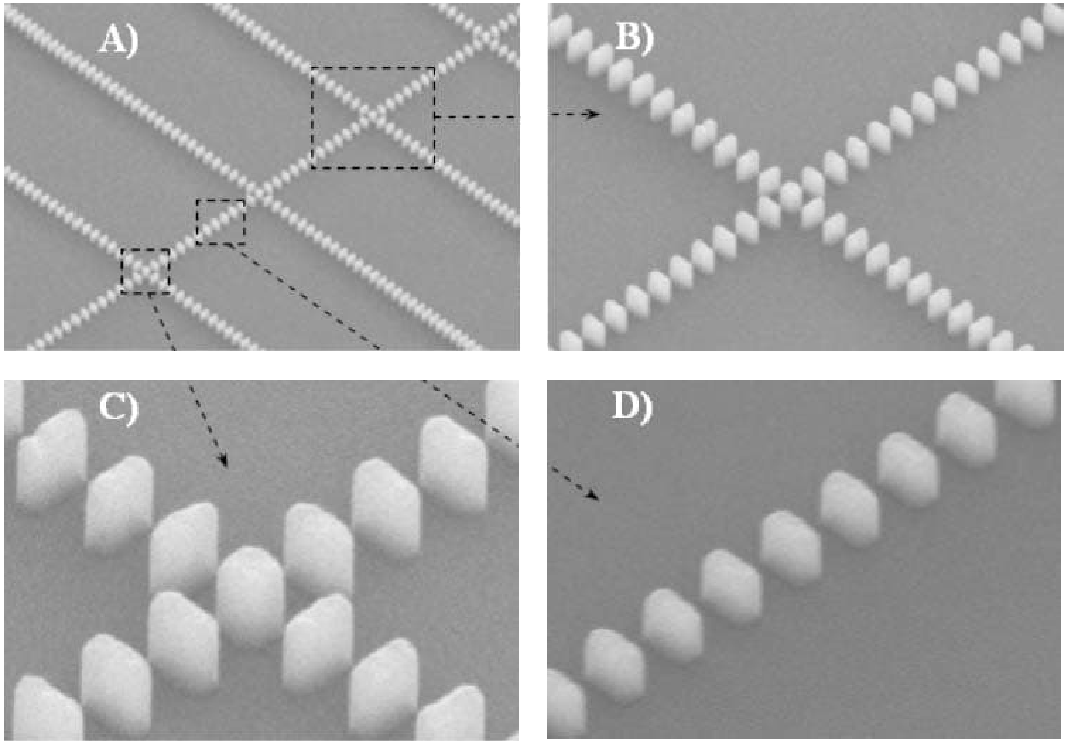

Scanning electron microscope images of SWG crossings:
A) multiple SWG crossings,
B) one SWG crossing,
C) detail of the crossing region with square center segment,
D) SWG straight waveguide.

P. J. Bock et al., Optics Express, 18(15), 16146 (2010).

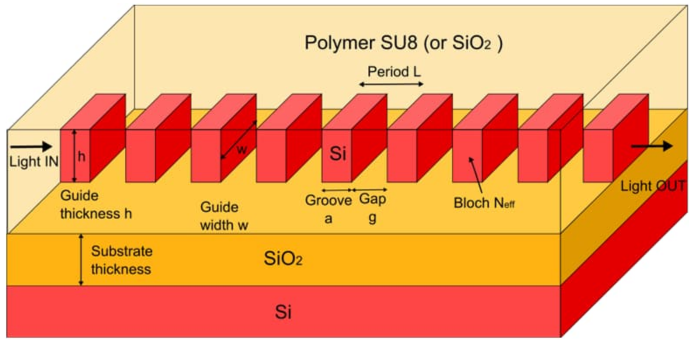

Disperzní vlastnosti SWG vlnovodů

Standard SWGW, w = 350 nm, Λ = 400 nm, g = 200 nm, TE polarization

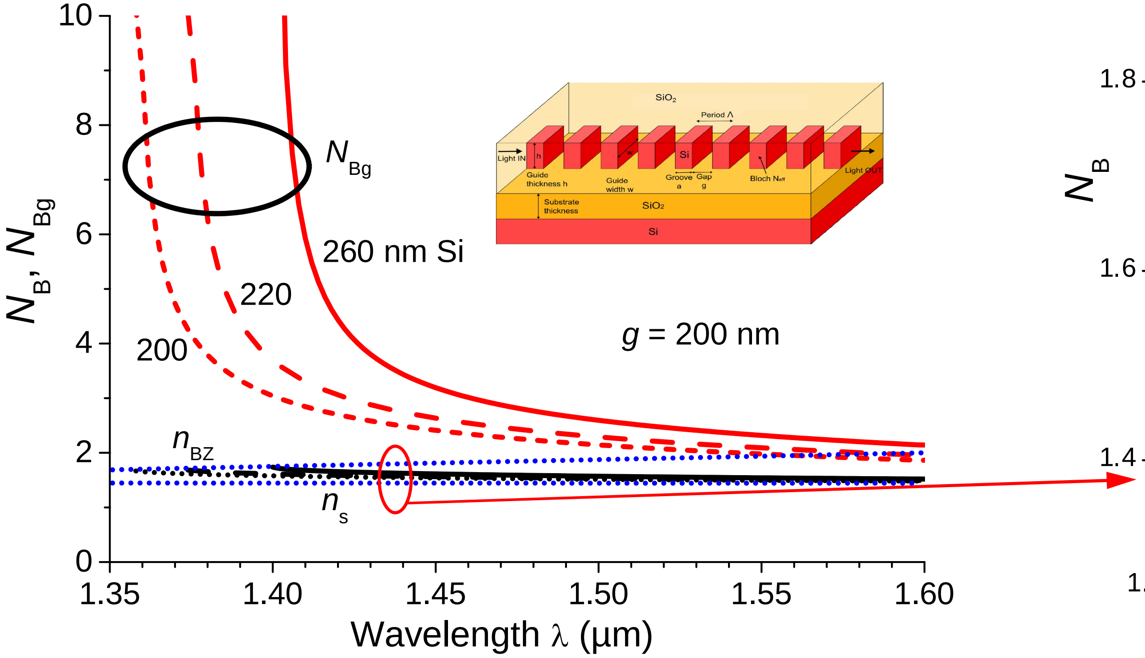

bandgap region

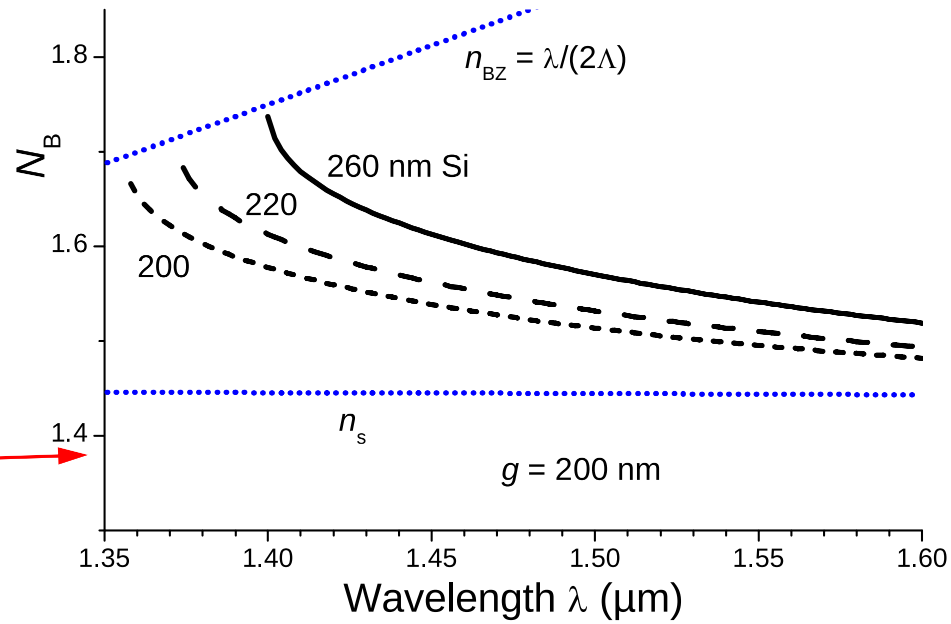

phase and group effective indices N_B , N_{Bg}

phase effective index N_B

Disperzní vlastnosti SWG vlnovodů

Standard SWGW, *w* = 350 nm, Λ = 400 nm, **various gap sizes** *g*, TE polarization

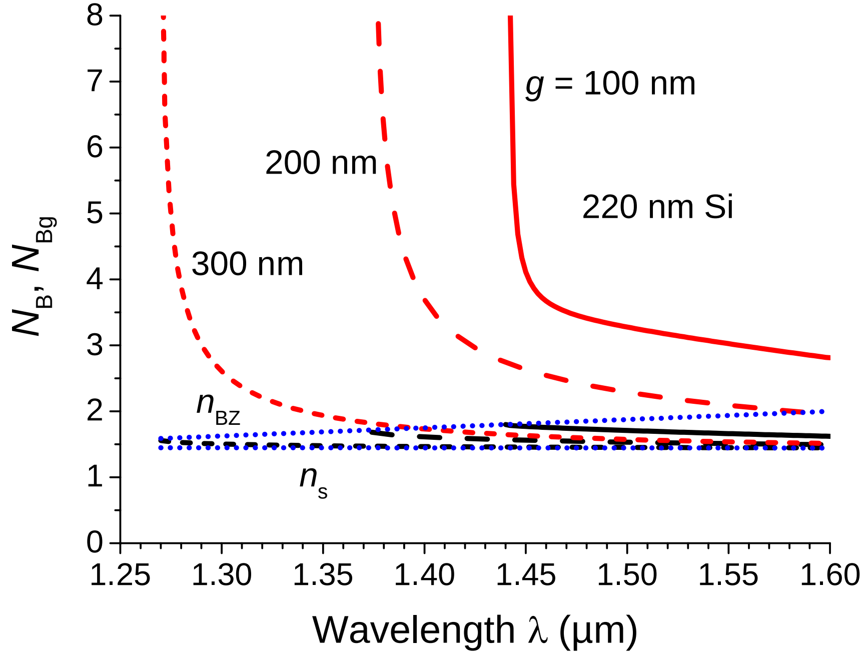

phase and group effective indices N_B , N_{Bg}

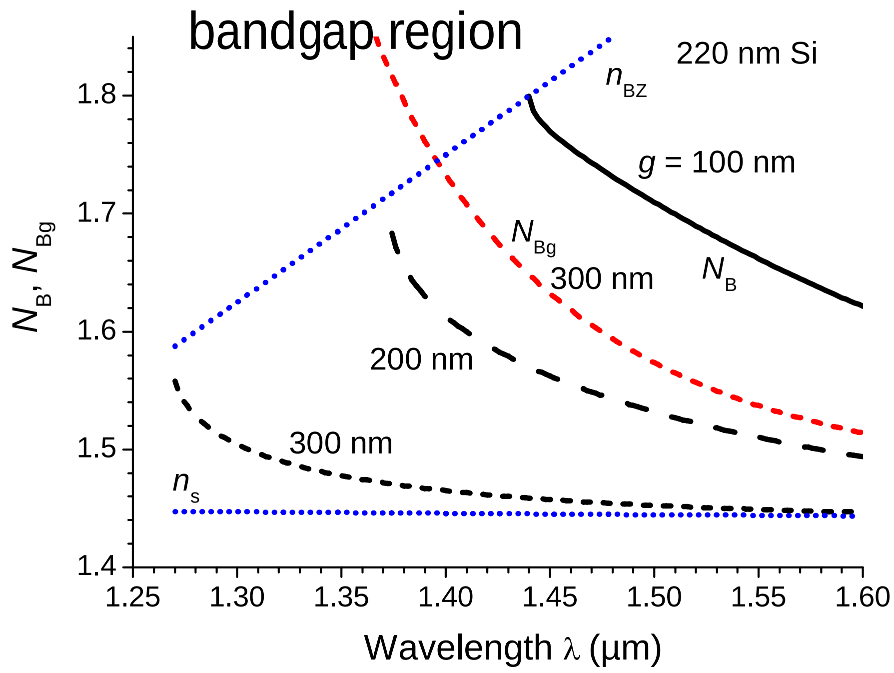

phase effective index N_B

Disperzní vlastnosti *štěrbinového* SWG vlnovodu

slot SWGW, width 2×200 nm+100 nm slot, Λ = 400 nm, *g* = 200 nm, TE polarization

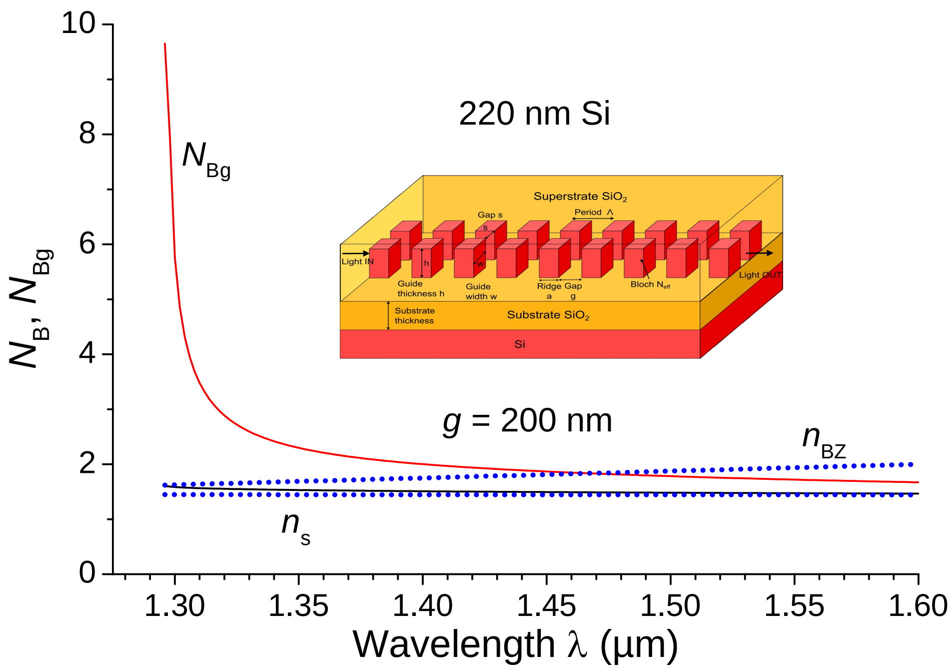

phase and group effective indices N_B , N_{Bg}

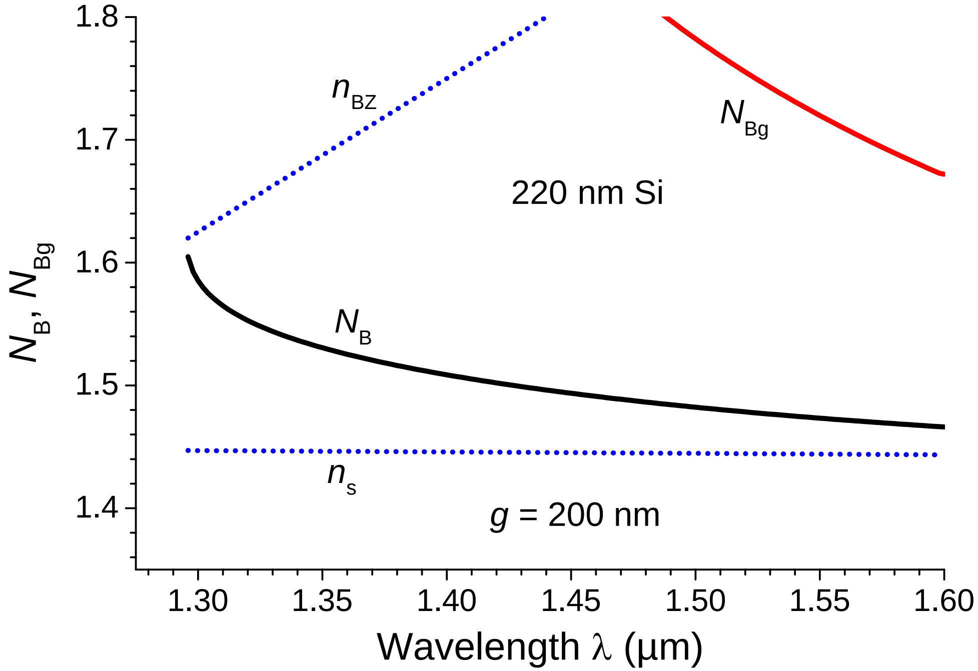

phase effective index N_B

POWER DENSITY DISTRIBUTION

standard SWG waveguide

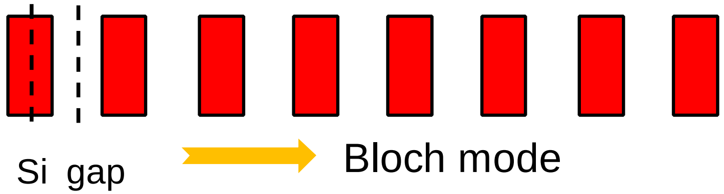

λ = 1.3 µm, *g* = 100 nm

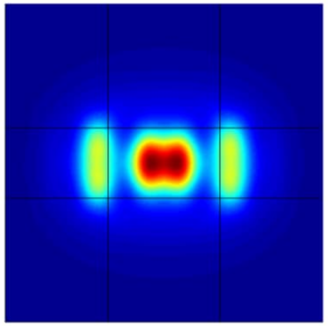

Si segment

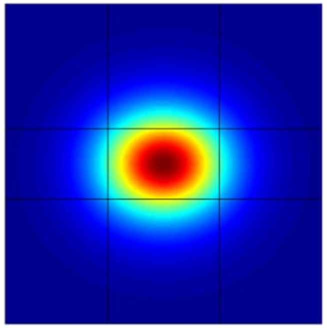

gap

λ = 1.55 µm, g = 360 nm
(Si filling fraction = 0.1)

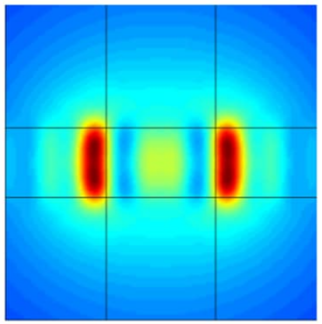

Si segment

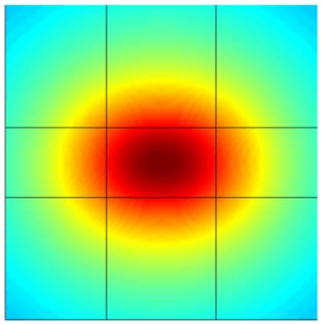

gap

slot SWG waveguide

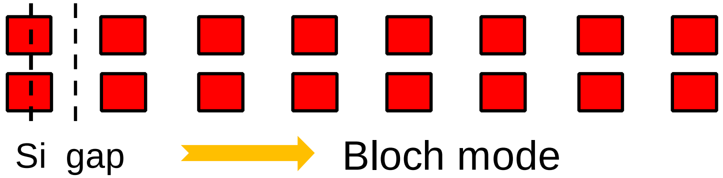

λ = 1.3 µm, *g* = 200 nm

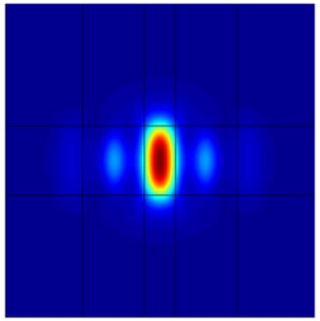

Si segment

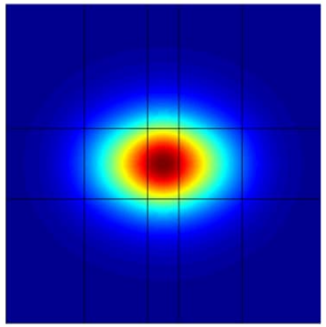

gap

Power of the Bloch mode of the slot SWG waveguide is ***very strongly*** localized in a low-index medium, similarly as a mode of a uniform slot waveguide

Field distribution of the Bloch mode of the SWG waveguide

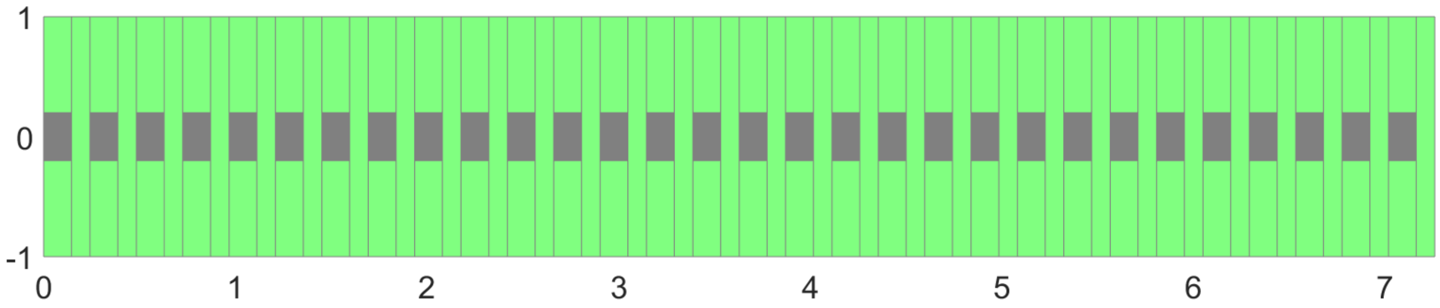

SWG vaveguide, top view
Si thickness *h* = 220 nm,
Si segments 400×145 nm^2,
SWG period 242 nm

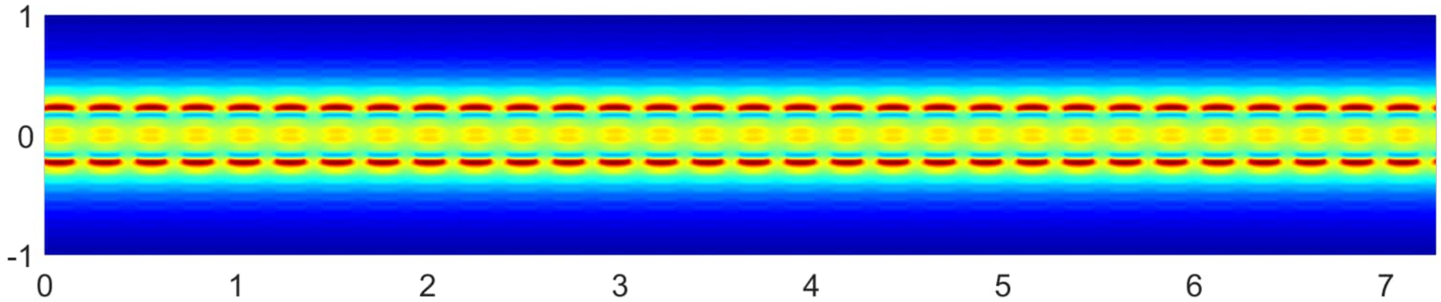

Dominant component
of the TE_{00} electric field,
$|E_x(x,z)|$, $\lambda = 1.55$ µm

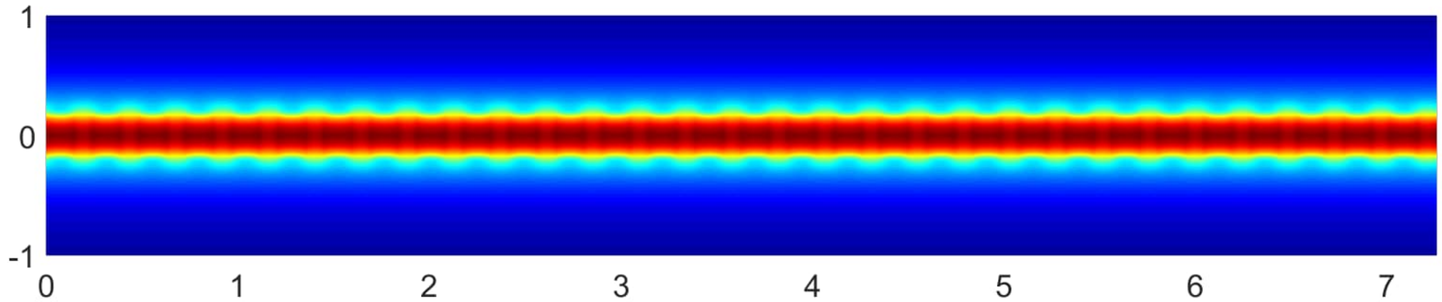

Dominant component
of the TE_{00} magnetic field,
$|H_y(x,z)|$

BLOCH MODE FIELD PROPAGATION

Vertical component of the magnetic field intensity @ λ = 1500 nm

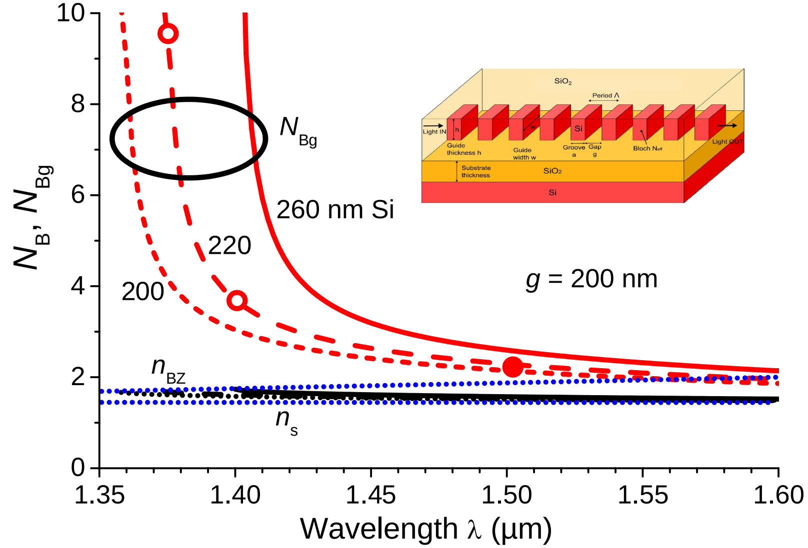

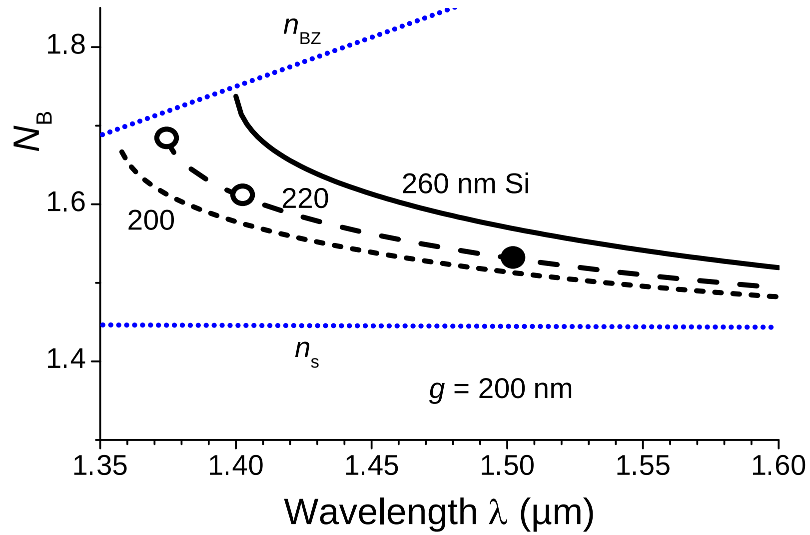

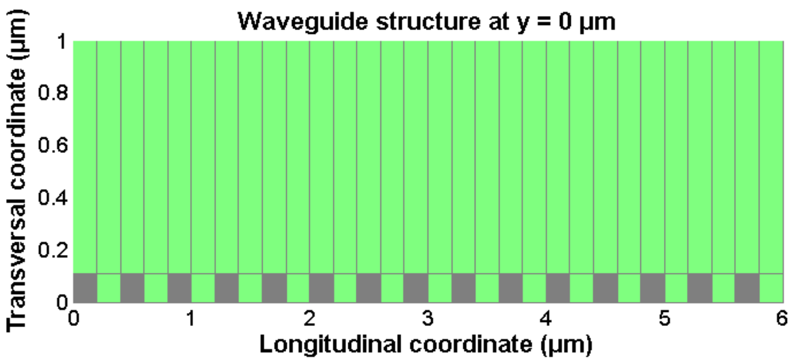

character quite similar
to a uniform waveguide

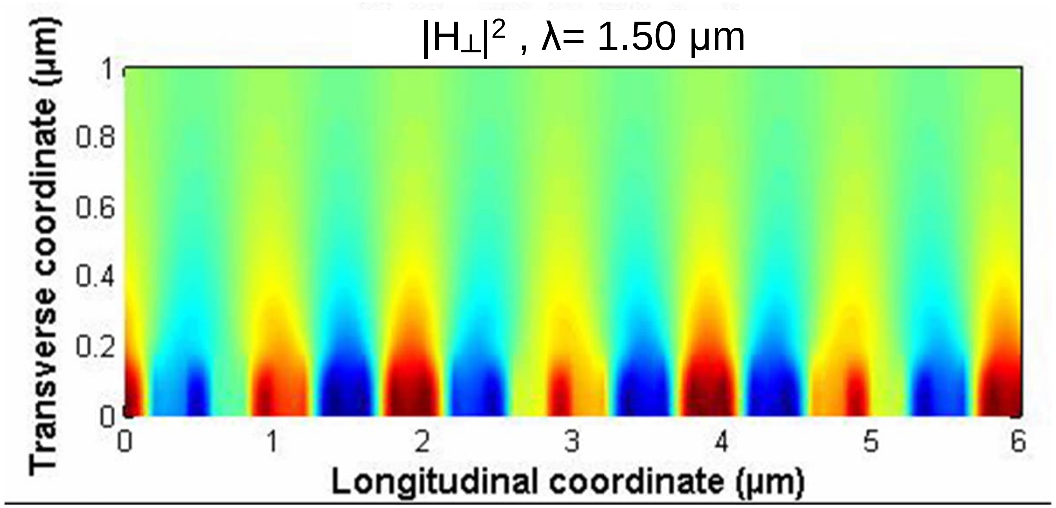

BLOCH MODE FIELD PROPAGATION

Vertical component of the magnetic field intensity @ λ = 1400 nm

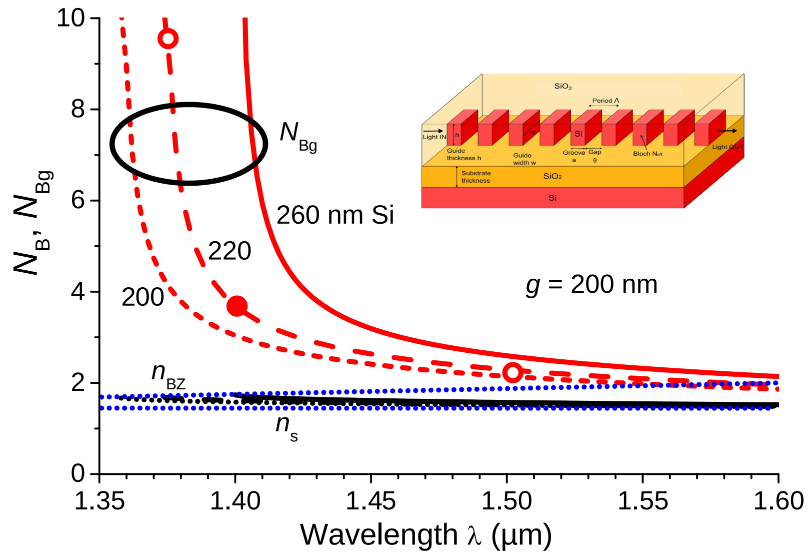

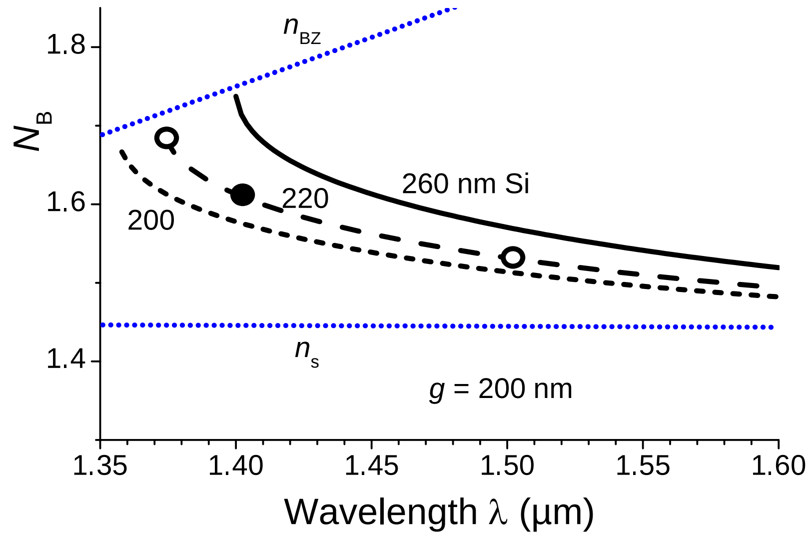

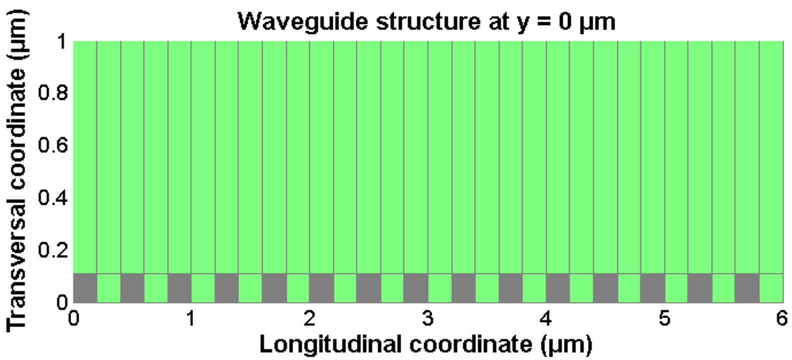

backward propagating waves are becoming important

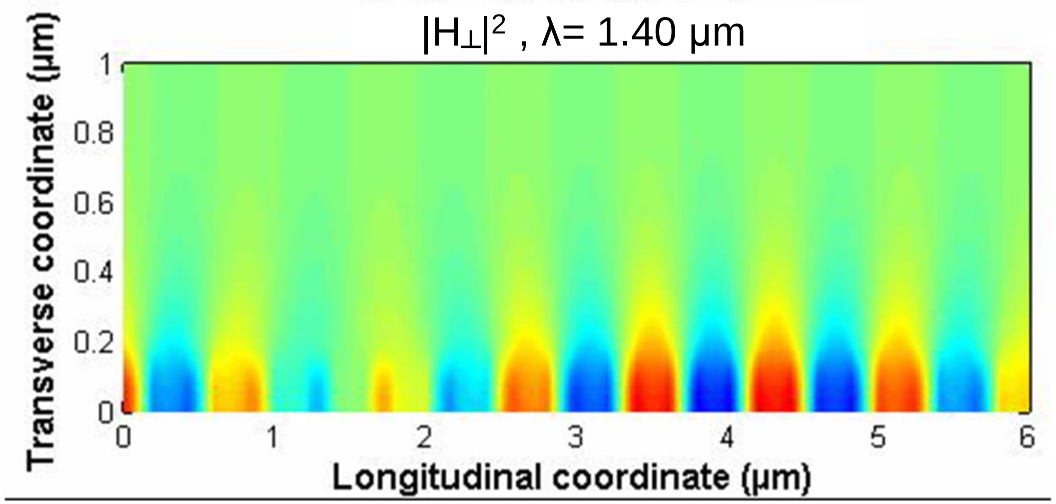

BLOCH MODE FIELD PROPAGATION

Vertical component of the magnetic field intensity @ λ = 1375 nm

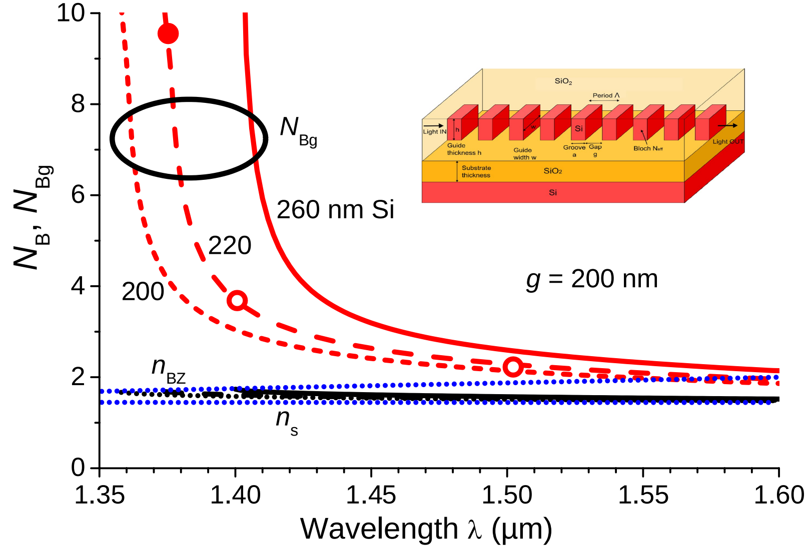

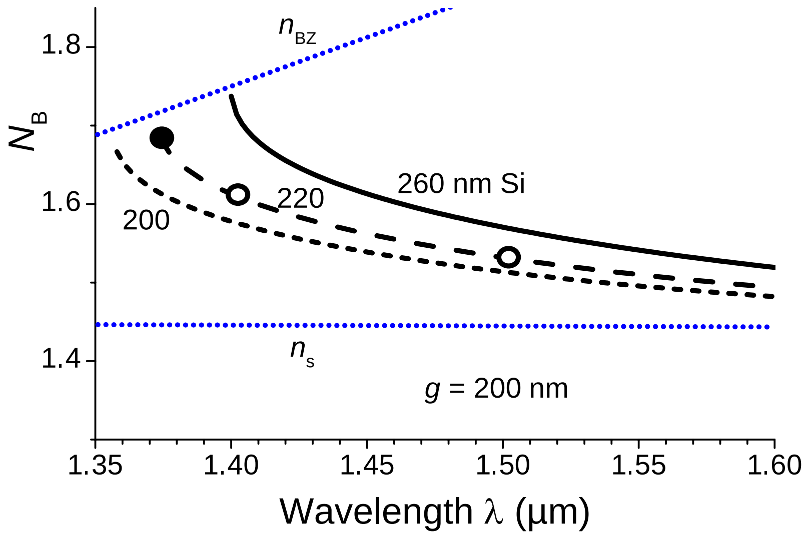

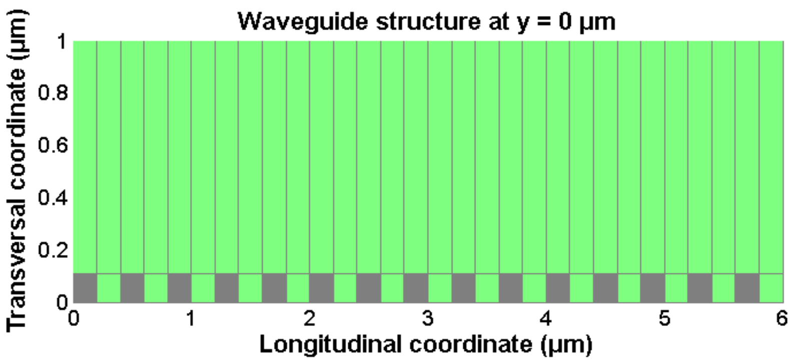

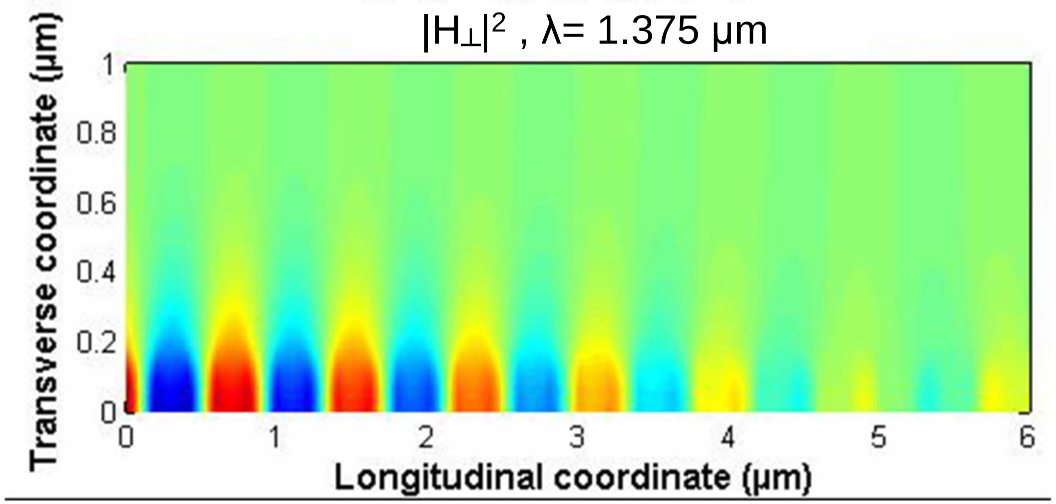

markedly resonant character

BLOCH MODE FIELD PROPAGATION

Vertical component of the magnetic field intensity @ λ = 1350 nm

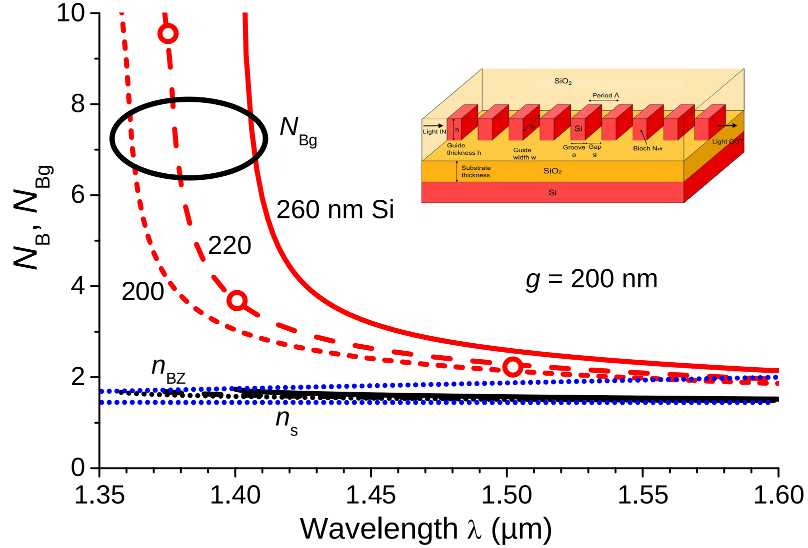

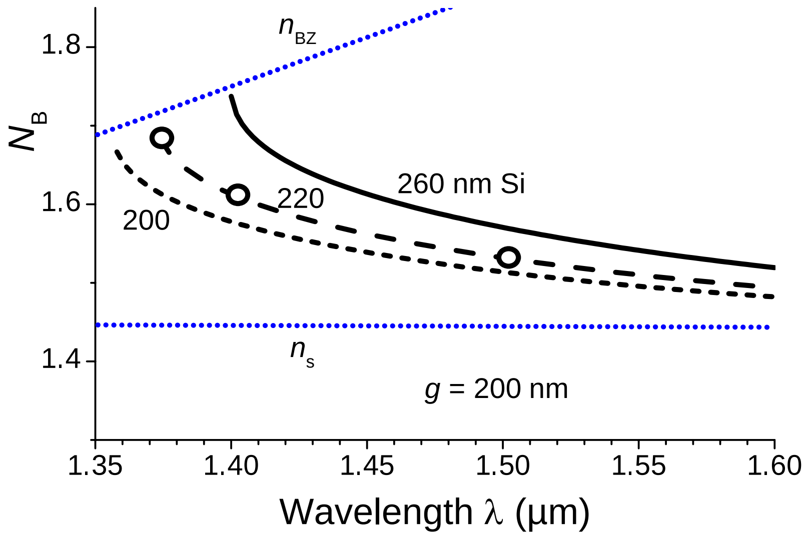

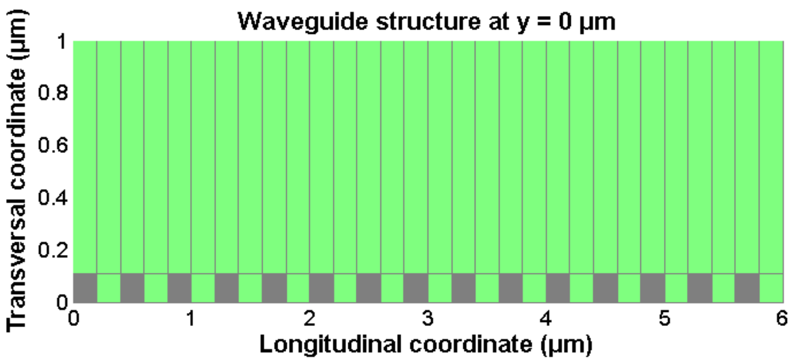

evanescent Bloch mode
within the bandgap

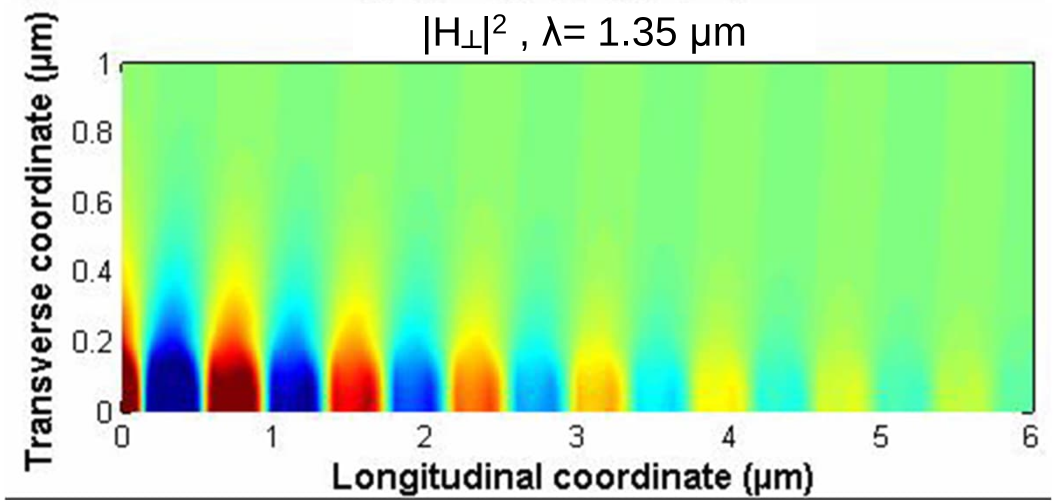

VAZBA MEZI SWG VLNOVODEM A NANODRÁTEM

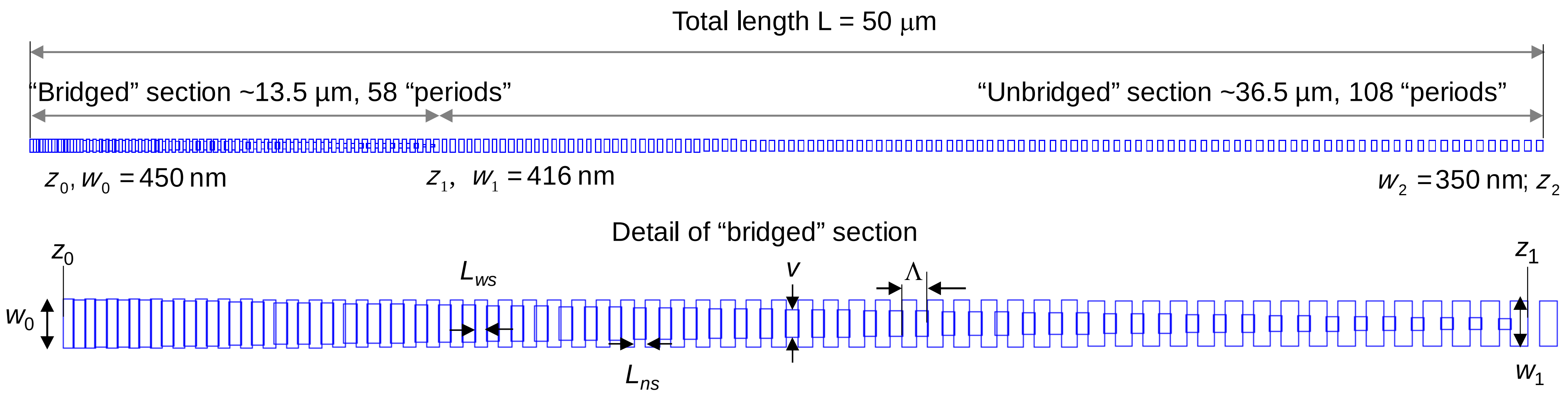

Both wide and narrow “bridged” segments are linearly tapered;
the period length Λ is also linearly tapered,
from 200 nm to 270 nm in the “bridged” section and
from 270 nm to 400 nm in the “unbridged” section

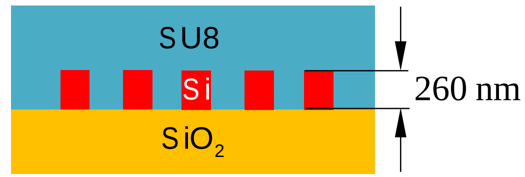

Version 2 (L/2)

Similar (linearly tapered) but twice shorter: total length ~ 25 μm

“Bridged” section ~ 6.75 μm, 29 “periods”, “unbridged” section ~ 18.25 μm, 54 “periods”

Version 3 (L/4)

Similar (linearly tapered) but four-times shorter: total length ~ 12.5 μm
“Bridged” section ~ 3.38 μm, 15 “periods”, “unbridged” section ~ 9.13 μm, 27 “periods”

Version 4 (L/8)

Similar (linearly tapered) but eight-times shorter: total length ~ 6.25 μm
“Bridged” section ~ 1.69 μm, 7 “periods”, “unbridged” section ~ 4.6 μm, 13 “periods”

TRANSMITTANCE AND REFLECTANCE OF THE NANOWIRE TO SWGW COUPLER

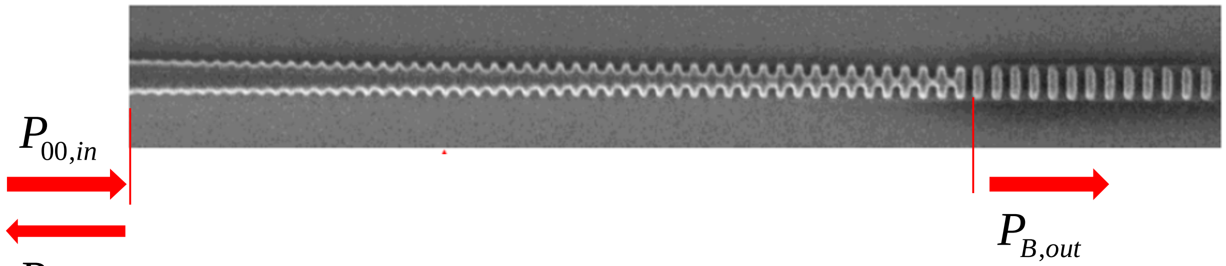

$$T = \frac{P_{B,out}}{P_{00,in}}, \quad R = \frac{P_{00,refl}}{P_{00,in}}$$

$P_{00,in}$, $P_{00,refl}$ … modal input and reflected power

$P_{B,out}$ … power of the fundamental forward Bloch mode

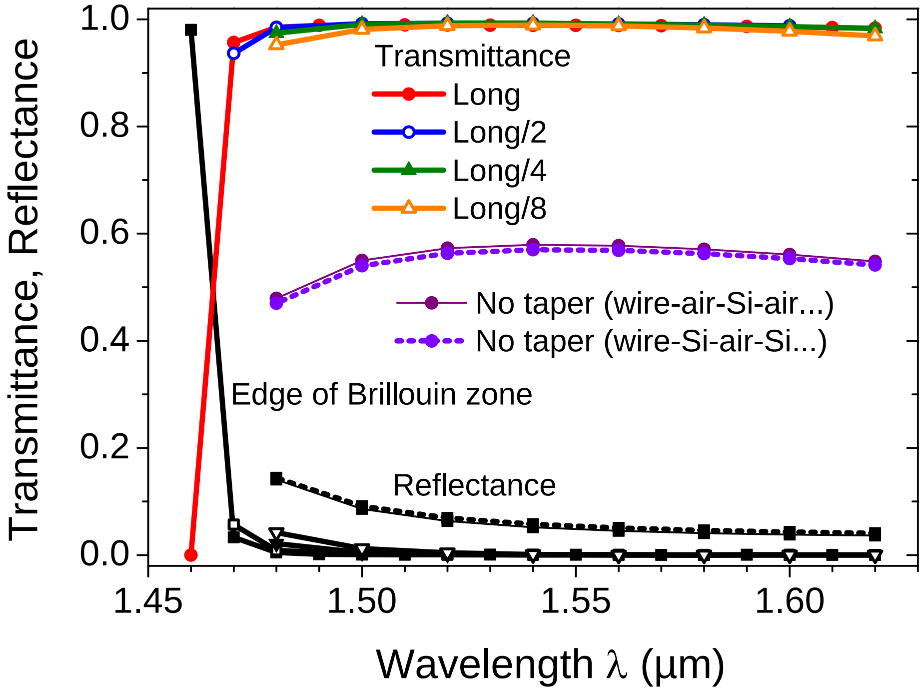

TE polarization

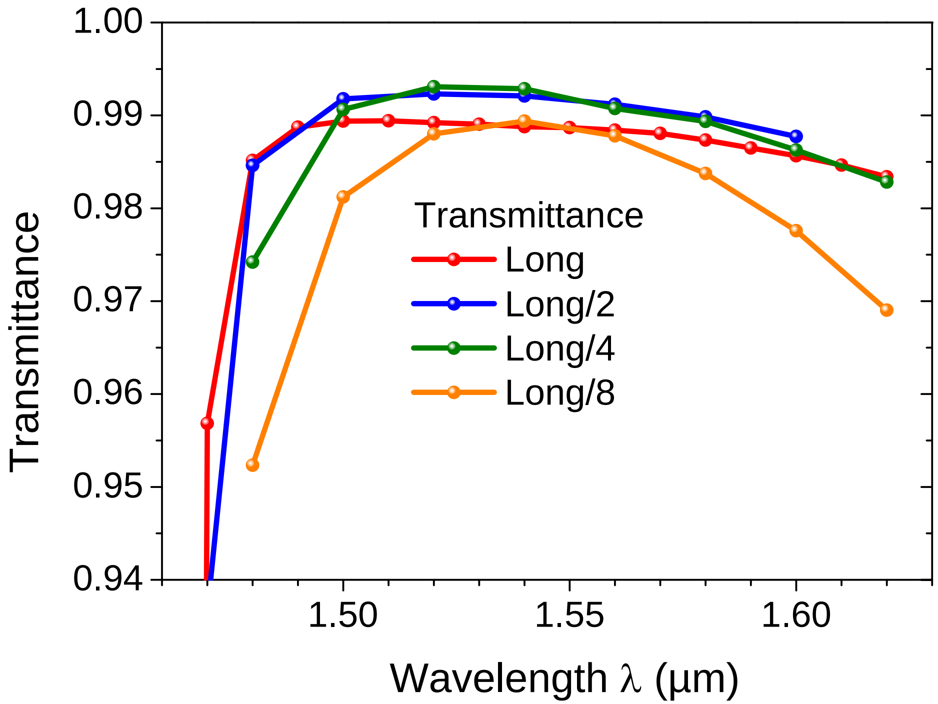

TRANSMITTANCE AND REFLECTANCE OF THE NANOWIRE TO SWGW COUPLER

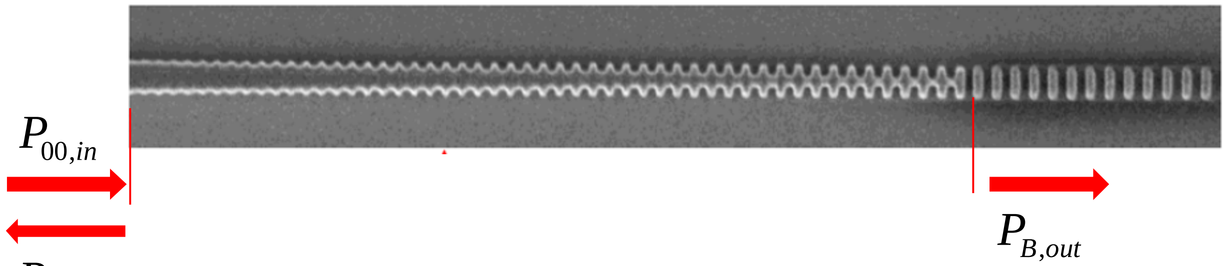

$$T = \frac{P_{B,out}}{P_{00,in}}, \quad R = \frac{P_{00,refl}}{P_{00,in}}$$

$P_{00,in}$, $P_{00,refl}$ … modal input and reflected power

$P_{B,out}$ … power of the fundamental forward Bloch mode

TE polarization

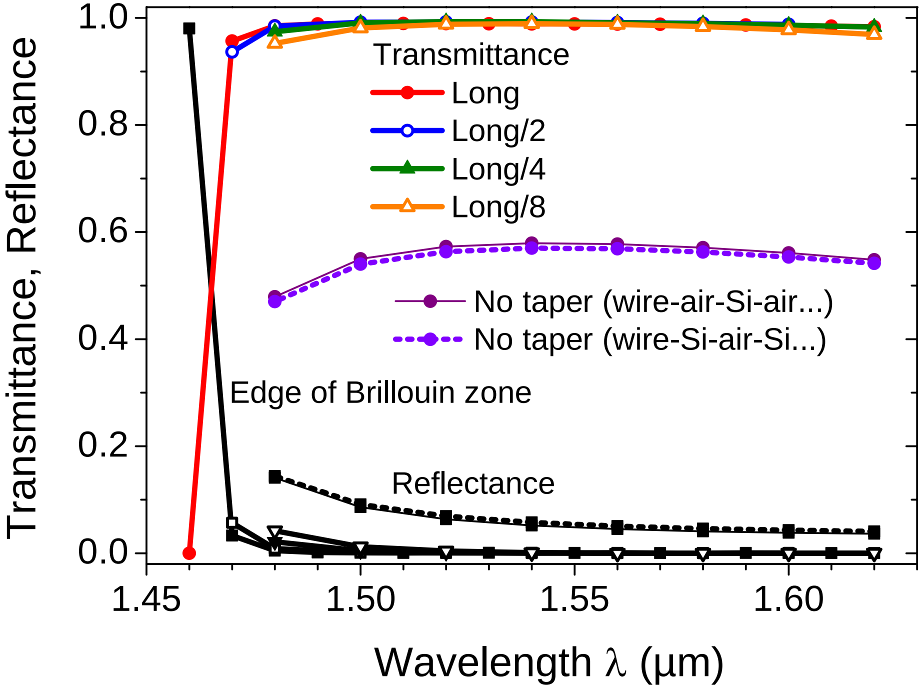

TM polarization

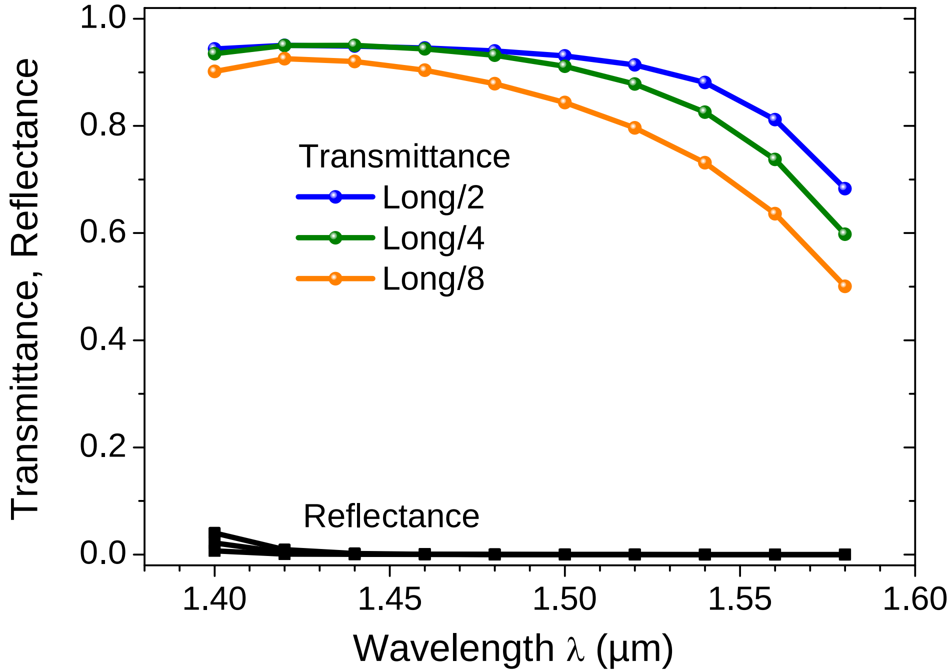

COUPLERS OF DIFFERENT LENGTHS

Version 1 (L)

vertical view; only upper half is shown because of structure symmetry

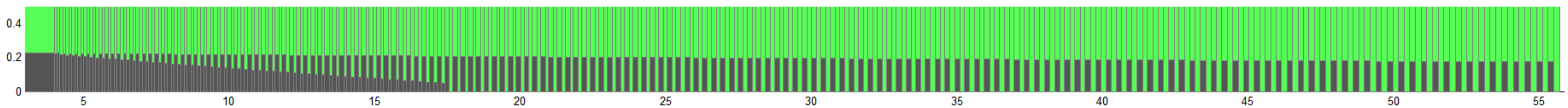

Version 2 (L/2)

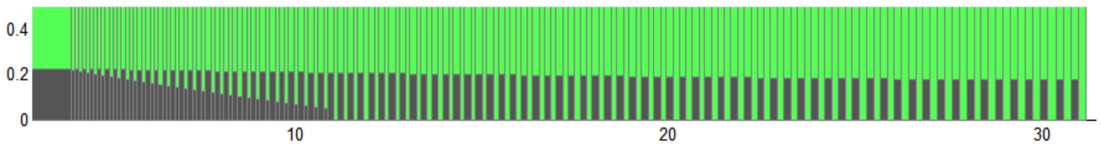

Version 3 (L/4)

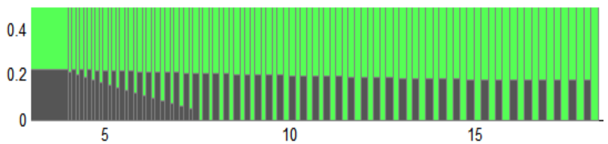

Version 4 (L/8)

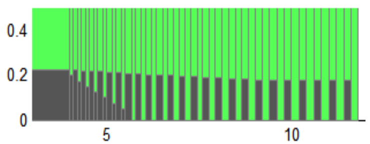

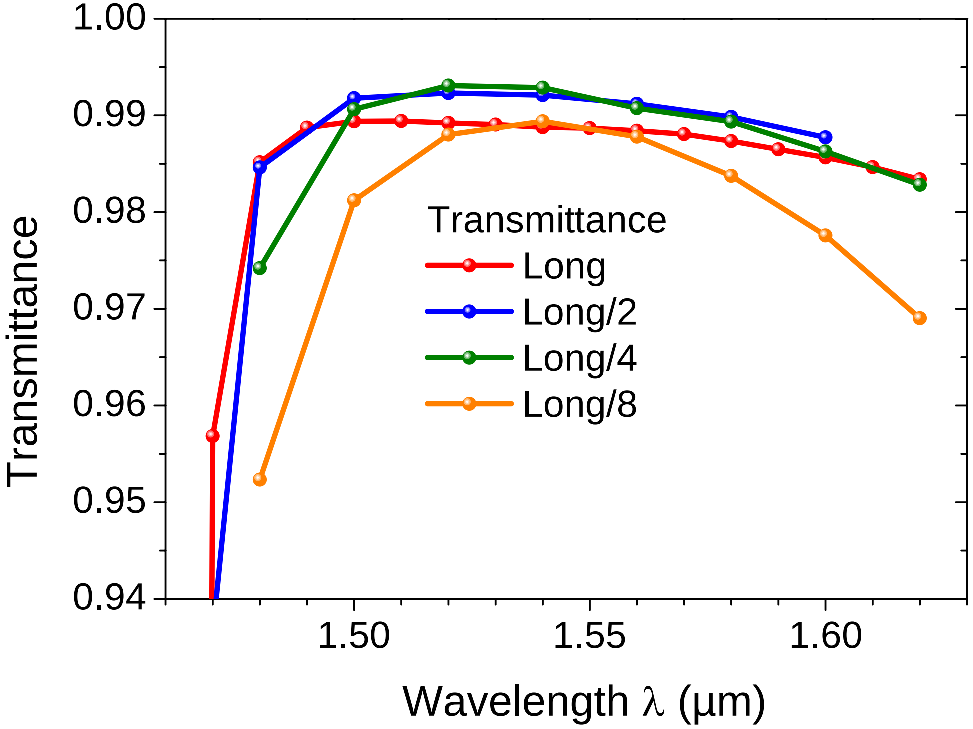

TE_{00} MODE FIELD DISTRIBUTION IN THE L/4 COUPLER: VERTICAL PLANE

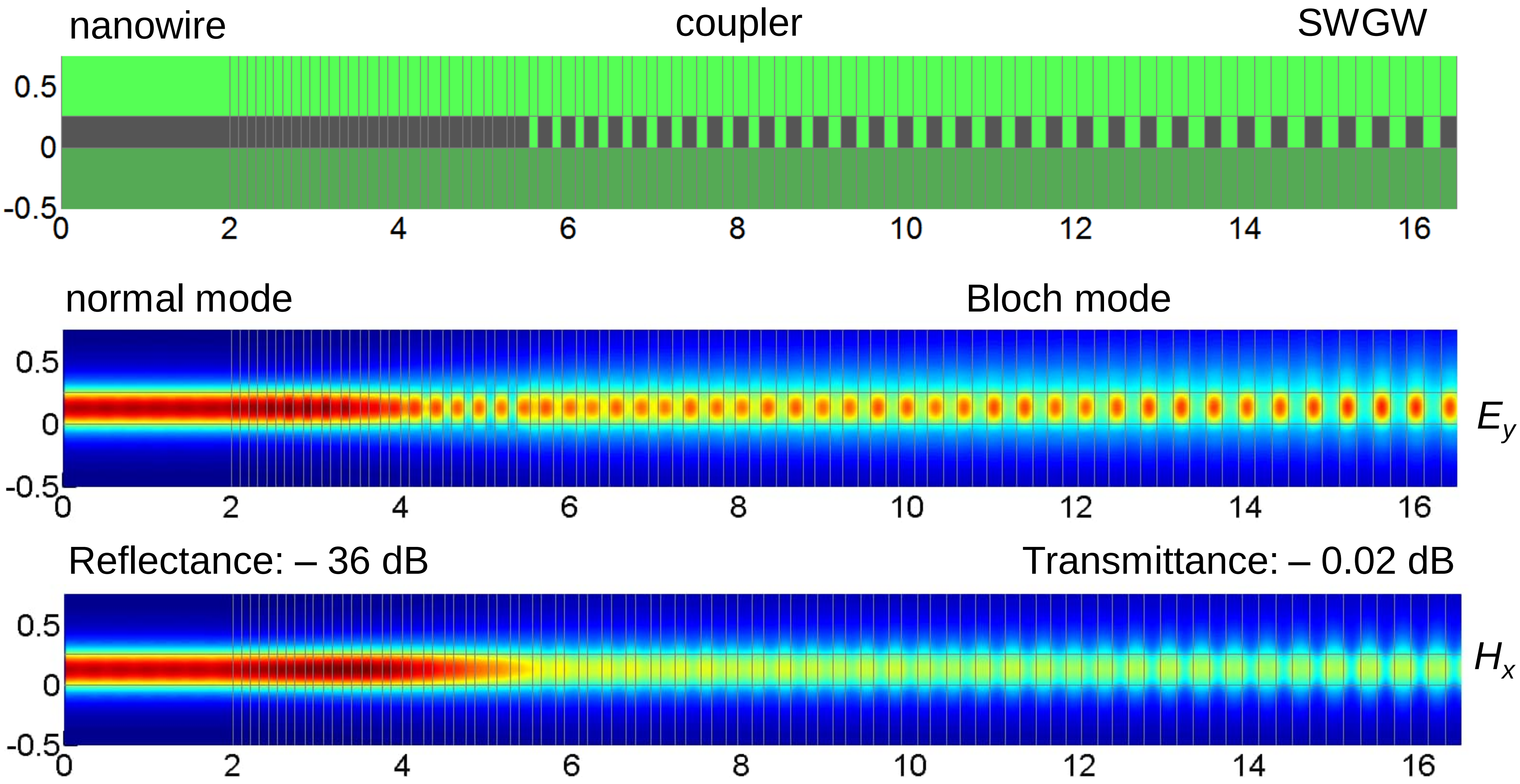

TE_{00} MODE FIELD DISTRIBUTION IN THE L/4 COUPLER: HORIZONTAL PLANE (upper half)

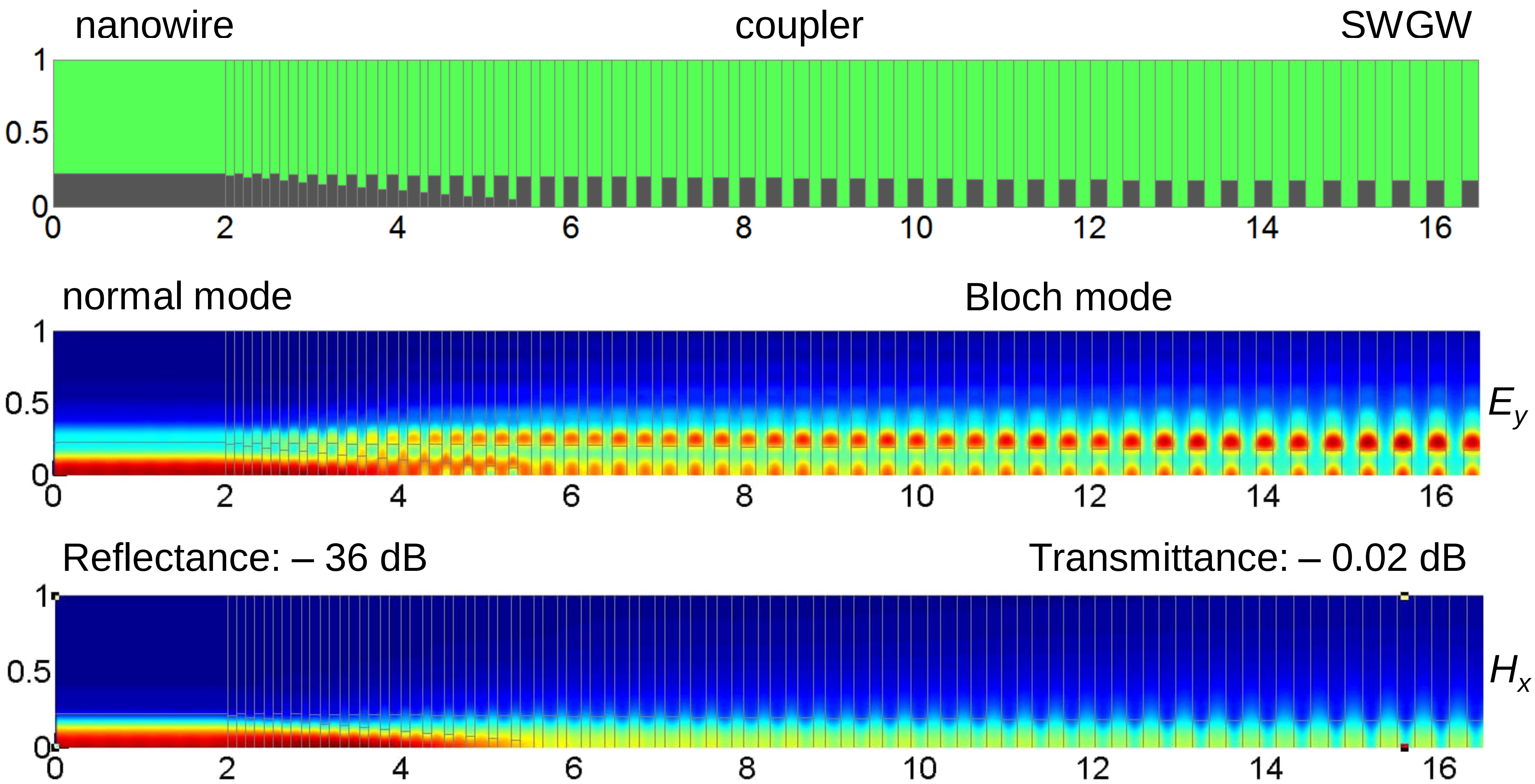

Aplikace subvlnových segmentovaných vlnovodů na optický konvertor vlnových délek

I. Glesk, P. J. Bock, P. Cheben *et al.*, Optics Express, 19 (15), 14031 (2011).

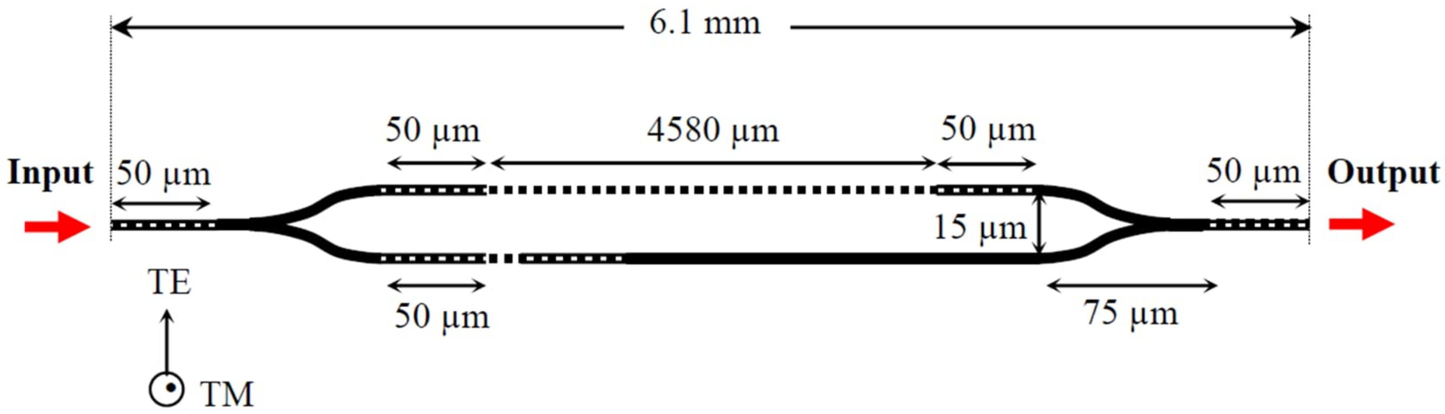

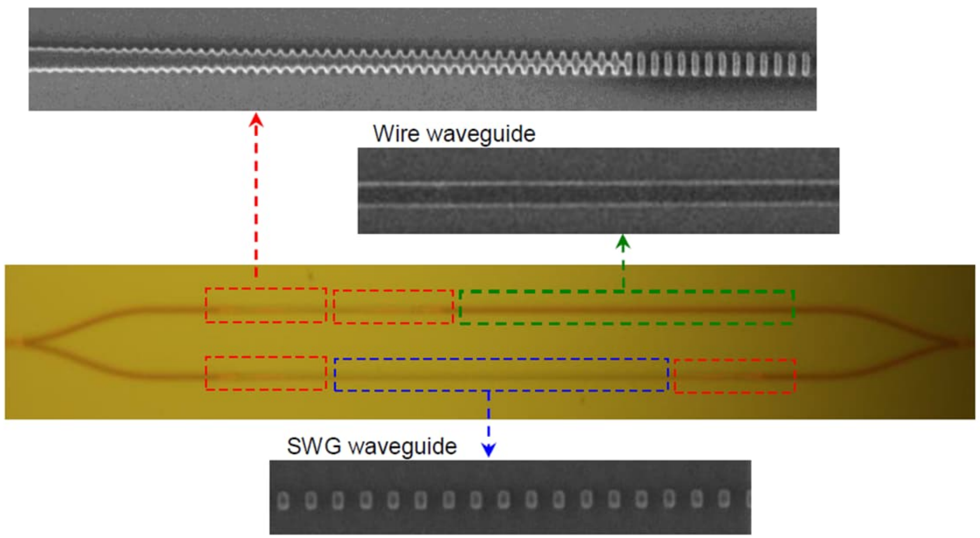

Vtipné využití rozdílu fázových a grupových rychlostí a optické lokalizace v jednotlivých větvích asymetrického MZ interferometru tvořeného v jedné větvi homogenním „fotonickým nanodrátem“ a ve druhé větvi „subvlnově segmenovaným“ vlnovodem k plně optickému spínání a konverzi vlnových délek se subpikosekundovou rychlostí

Aplikace subvlnových segmentovaných vlnovodů na směrovou odbočnici

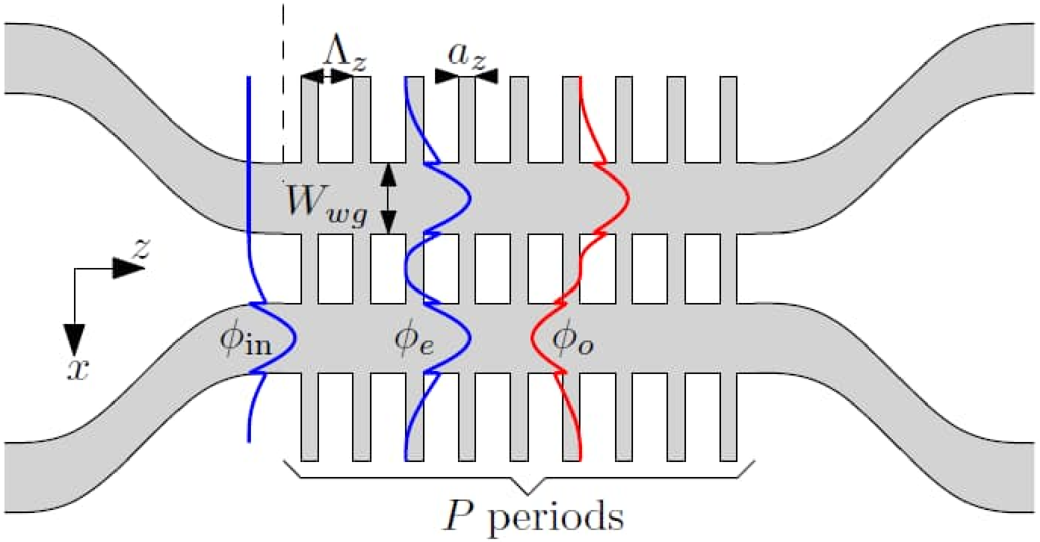

„Vložný útlum“
v obou větvích

Optimalizace parametrů
umožňuje využít
větší šířku pásma:

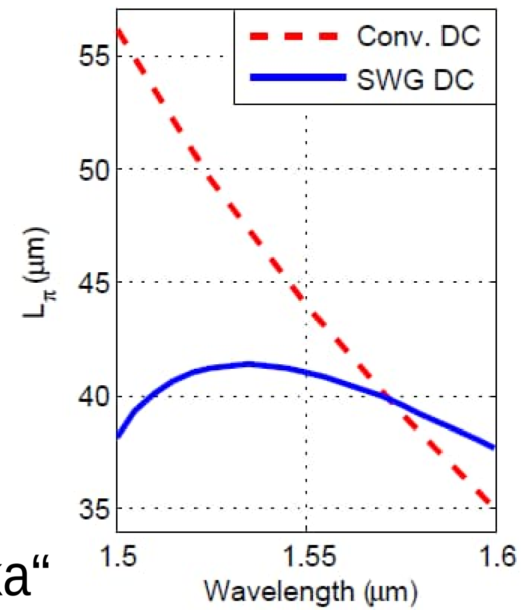

„Vazební délka“

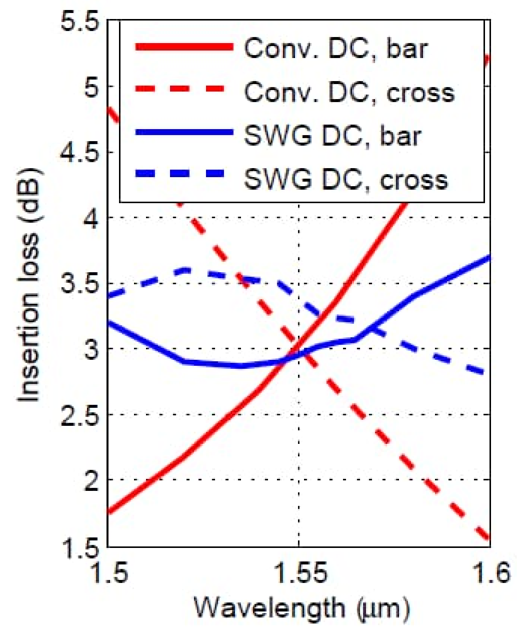

Aplikace subvlnových segmentovaných vlnovodů na vazební člen s mnohovidovou interferencí

P. Cheben et al., Wavelength-Independent Multimode Interference Coupler, Opt. Express 2012
NRC, Ottawa, Canada, and University of Malaga, Spain

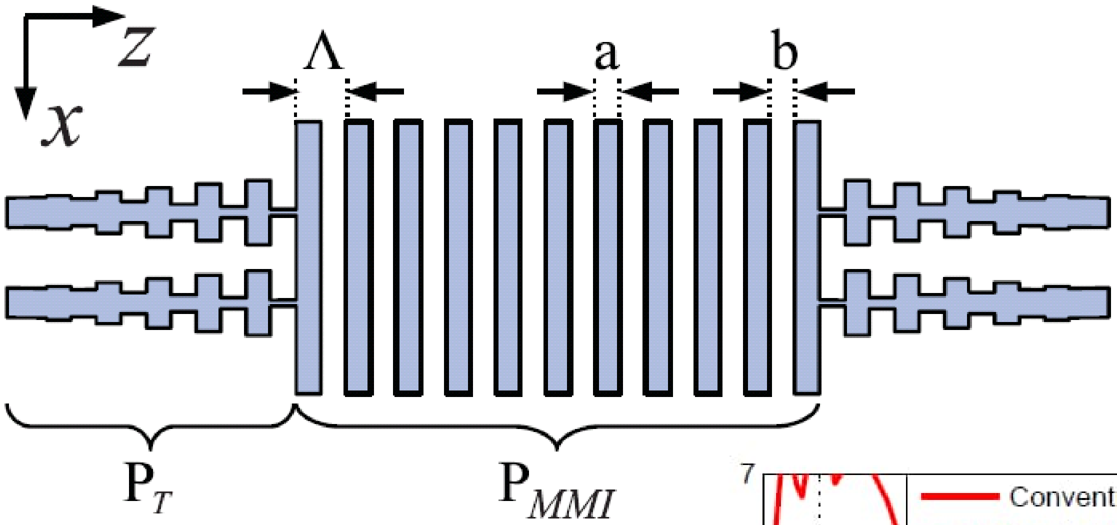

Optimalizace parametrů umožňuje širokopásmové použití

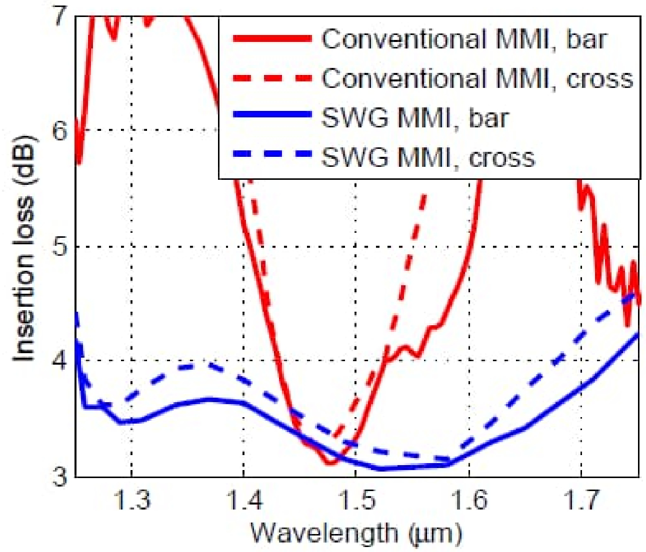

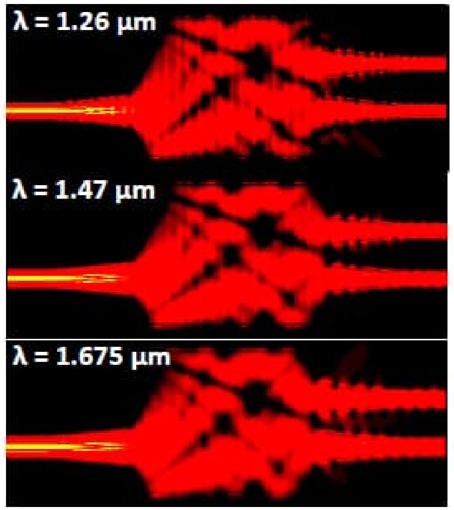

INFLUENCE OF RANDOM FLUCTUATIONS ON SWGW PERFORMANCE

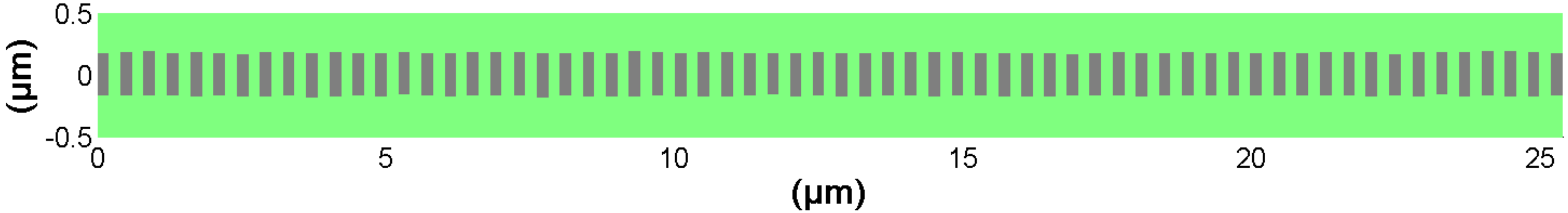

Positions and dimensions of Si segments fluctuate with normal distribution and standard deviation σ

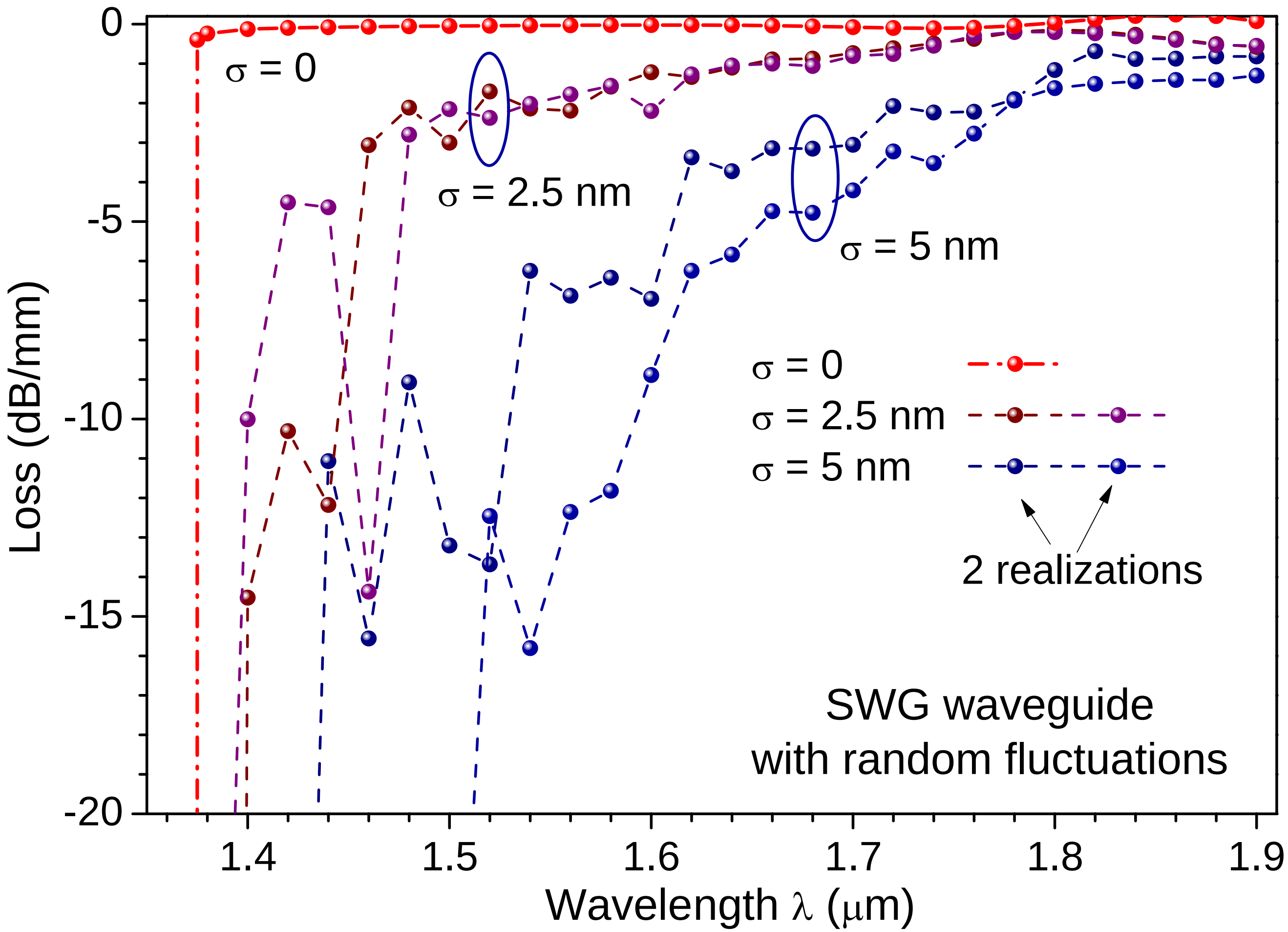

INFLUENCE OF RANDOM FLUCTUATIONS ON SWGW COUPLER PERFORMANCE

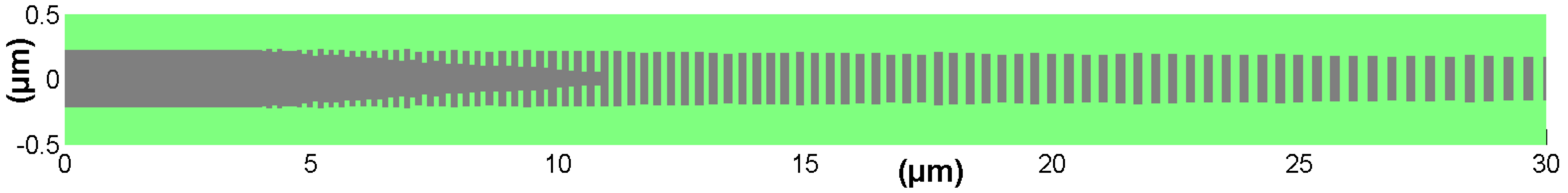

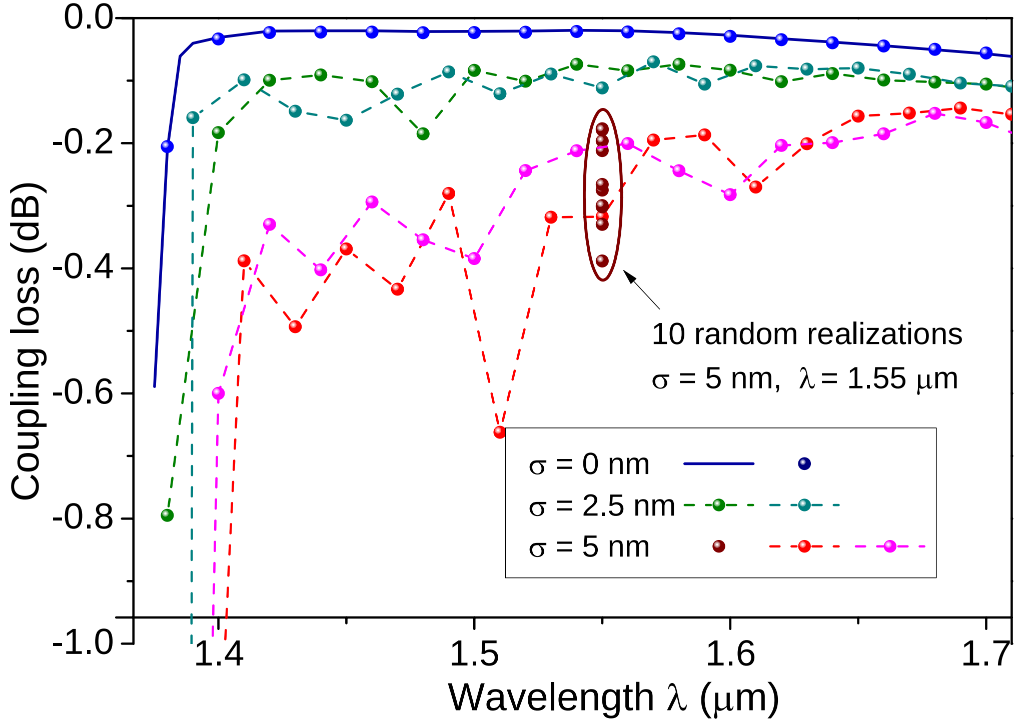

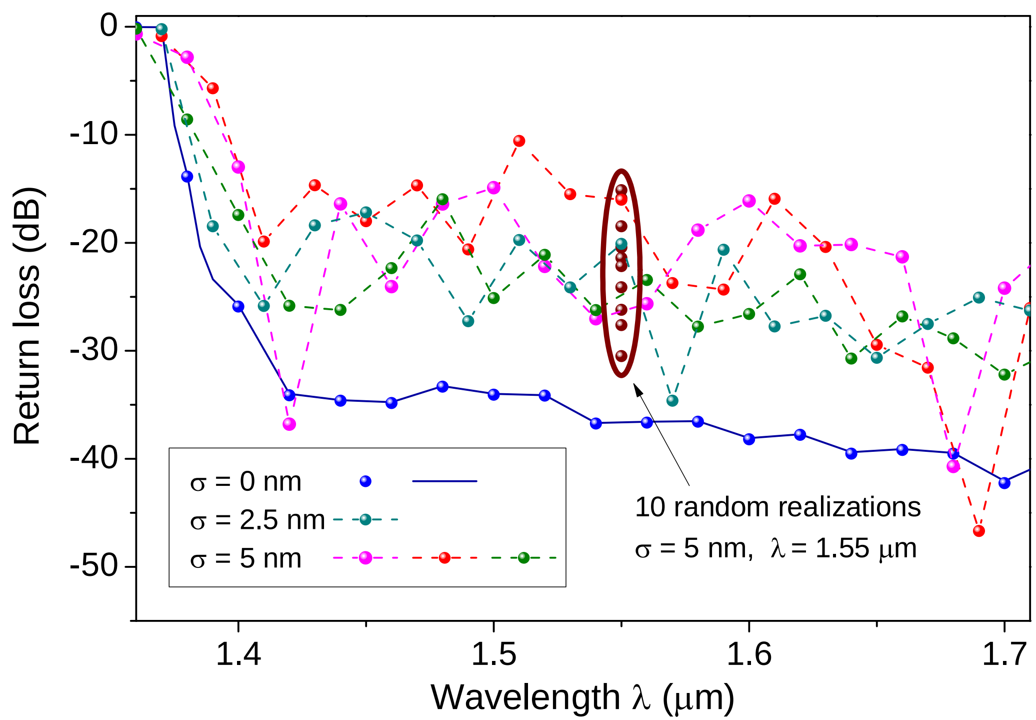

BROADBAND SWGW MMI COUPLER

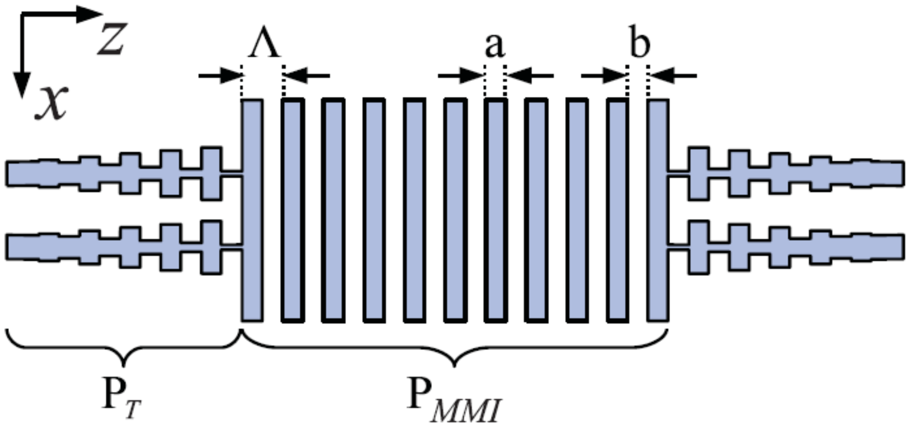

1. Optimization of MMI section for broadband operation
2. Check of imaging properties of the MMI section
3. Verification of taper function
4. Analysis of possible mutual coupling between tapers
5. Field distribution and scattering matrix
   of the complete coupler

A. Maese-Novo, R. Halir, S. Romero-García, D. Pérez-Galacho, L. Zavargo-Peche, A. Ortega-Moñux,
I. Molina-Fernández, J. G.Wangüemert-Pérez, and P. Cheben, *Opt. Express* vol 21, 7033-7040 (2013)

BLOCH MODES IN THE SWG MULTIMODE REGION

$\left|E_y(x,y)\right|, \quad \lambda = 1.55\ \mu\text{m}$

$\Lambda = 180\ \text{nm}$

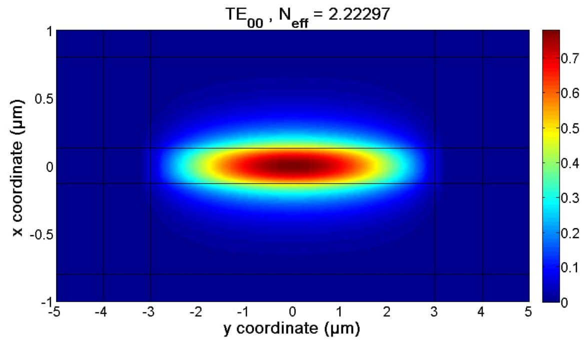

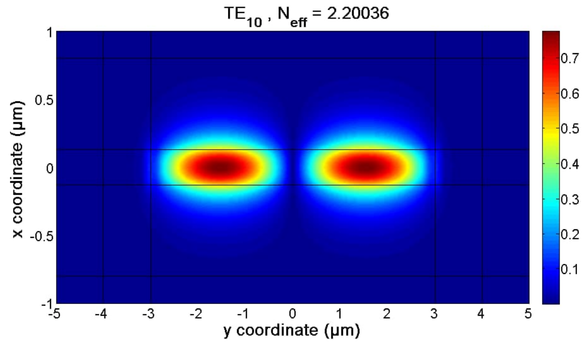

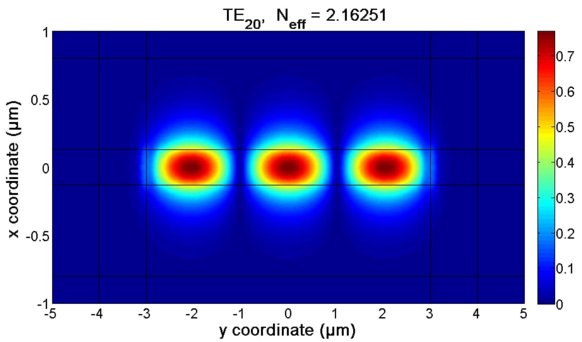

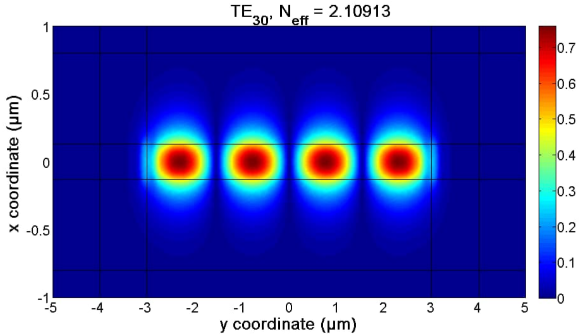

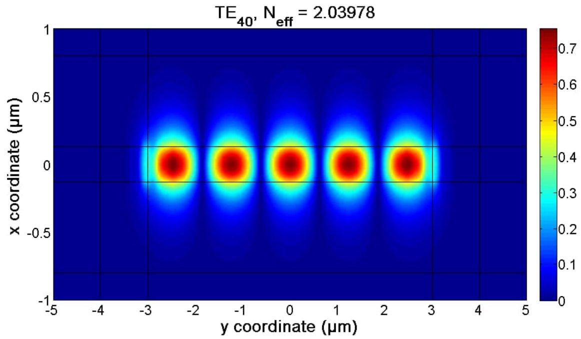

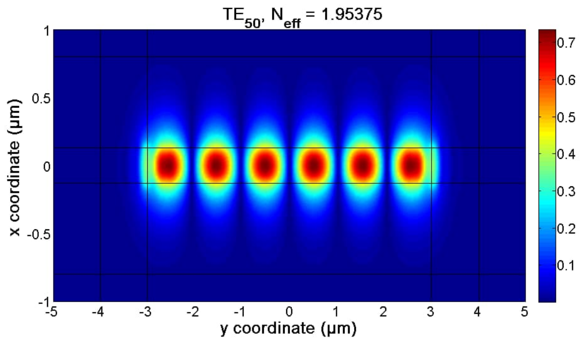

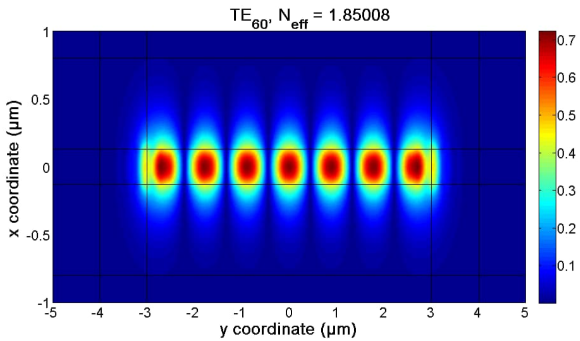

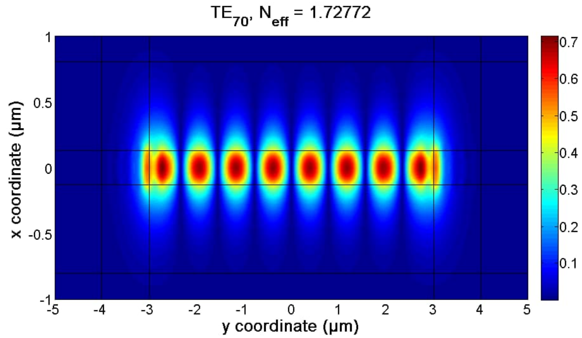

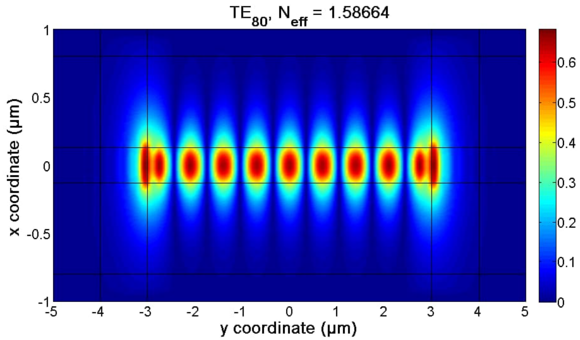

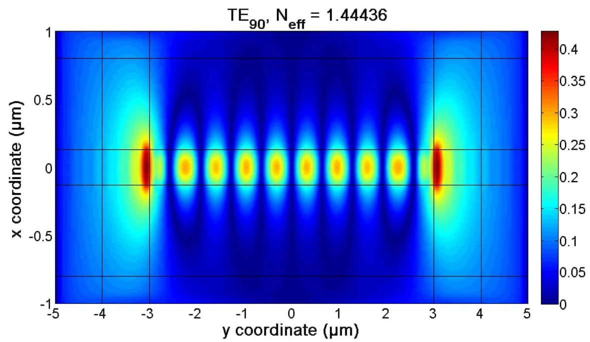

TE_{90} mode is weakly guided and for $\lambda > 1.55\ \mu\text{m}$ is cut-off

OPTIMIZATION OF MMI SECTION FOR BROADBAND OPERATION

Minimize wavelength dependence of the beat length between several lowest-order lateral Bloch modes by optimization of period length; MMI section width = 6 μm

$$\text{"ideal" beat length:}\quad L_{\pi m} = \frac{\left[(m+1)^2 - 1\right]\pi}{3(\beta_0 - \beta_m)} = \frac{m(m+2)}{6(N_{00} - N_{0m})},\quad m = 1,\ 2,\ \ldots,\ 8$$

Eff. indices

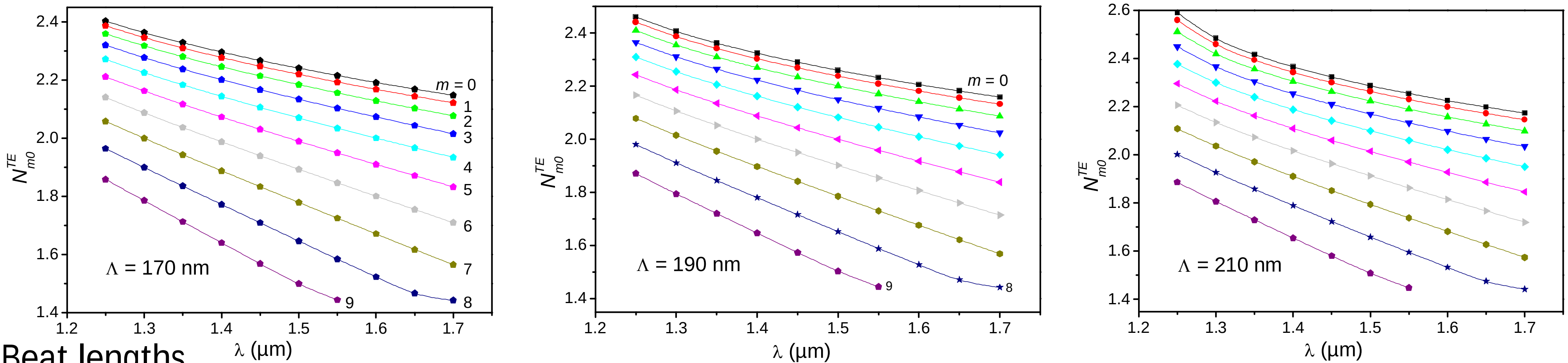

Beat lengths

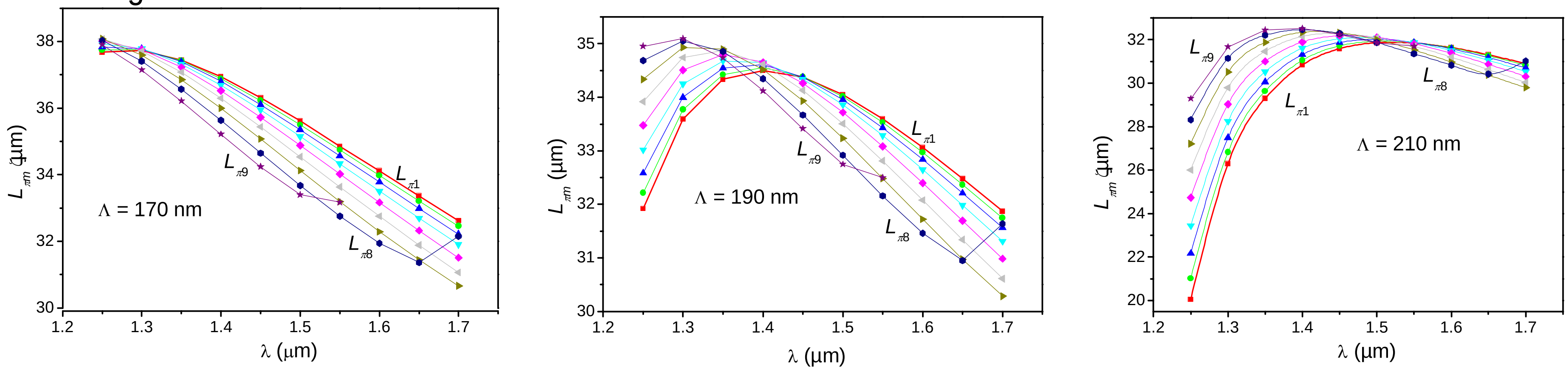

OPTIMIZATION OF THE MMI SECTION FOR 1.3 – 1.7 μm WAVELENGTH RANGE

Average beat lengths

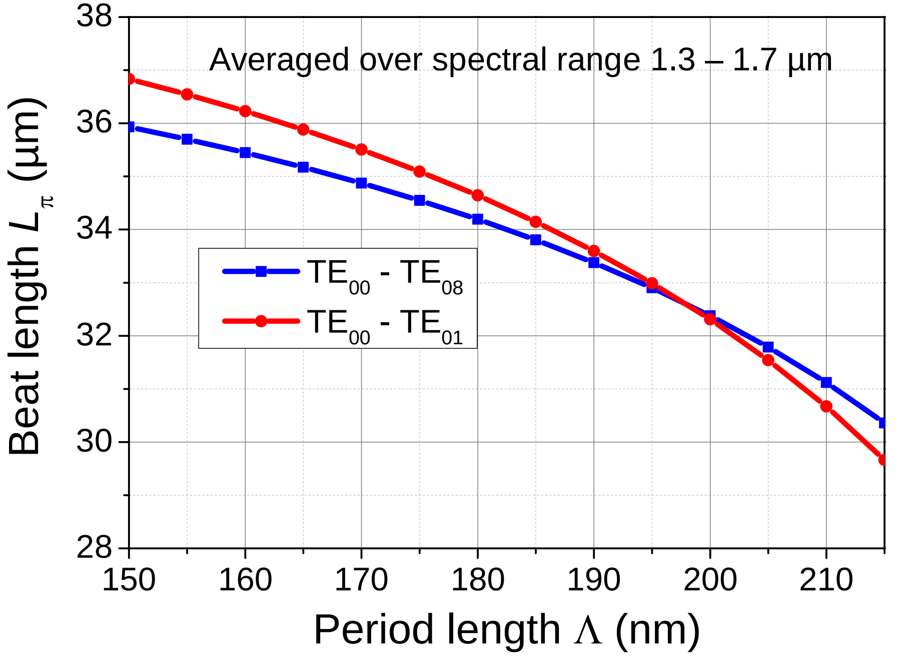

Standard deviations of the beat lengths

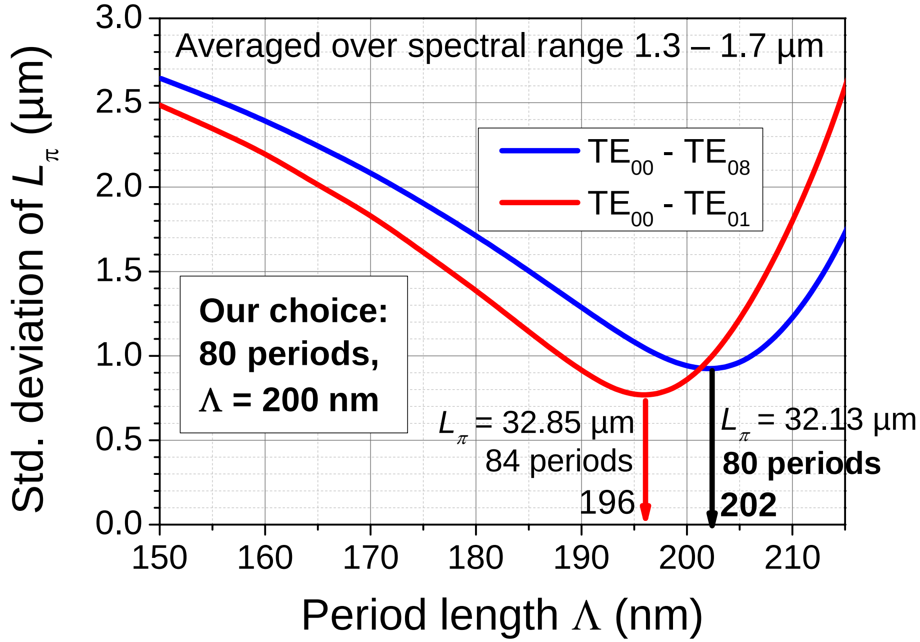

Averaging over wavelengths and modes:

$$\Lambda_{opt}^{0-1} = 196\text{ nm},\quad L_\pi^{0-1} = 32.85\ \mu\text{m},\quad NoP^{0-1} \doteq L_\pi^{0-1} \big/ (2\Lambda_{opt}^{0-1}) = 84\ \text{periods},$$

$$\Lambda_{opt}^{0-8} = 202\text{ nm},\quad L_\pi^{0-8} = 32.13\ \mu\text{m},\quad NoP^{0-8} \doteq L_\pi^{0-8} \big/ (2\Lambda_{opt}^{0-8}) = 80\ \text{periods}.$$

IMAGING PROPERTIES OF THE SWG MMI SECTION

Excitation of the SWG MMI section with SWG “ports”
by the superposition of symmetric and antisymmetric Bloch modes

MMI: 80 periods, Λ = 200 nm

$|E_y|$

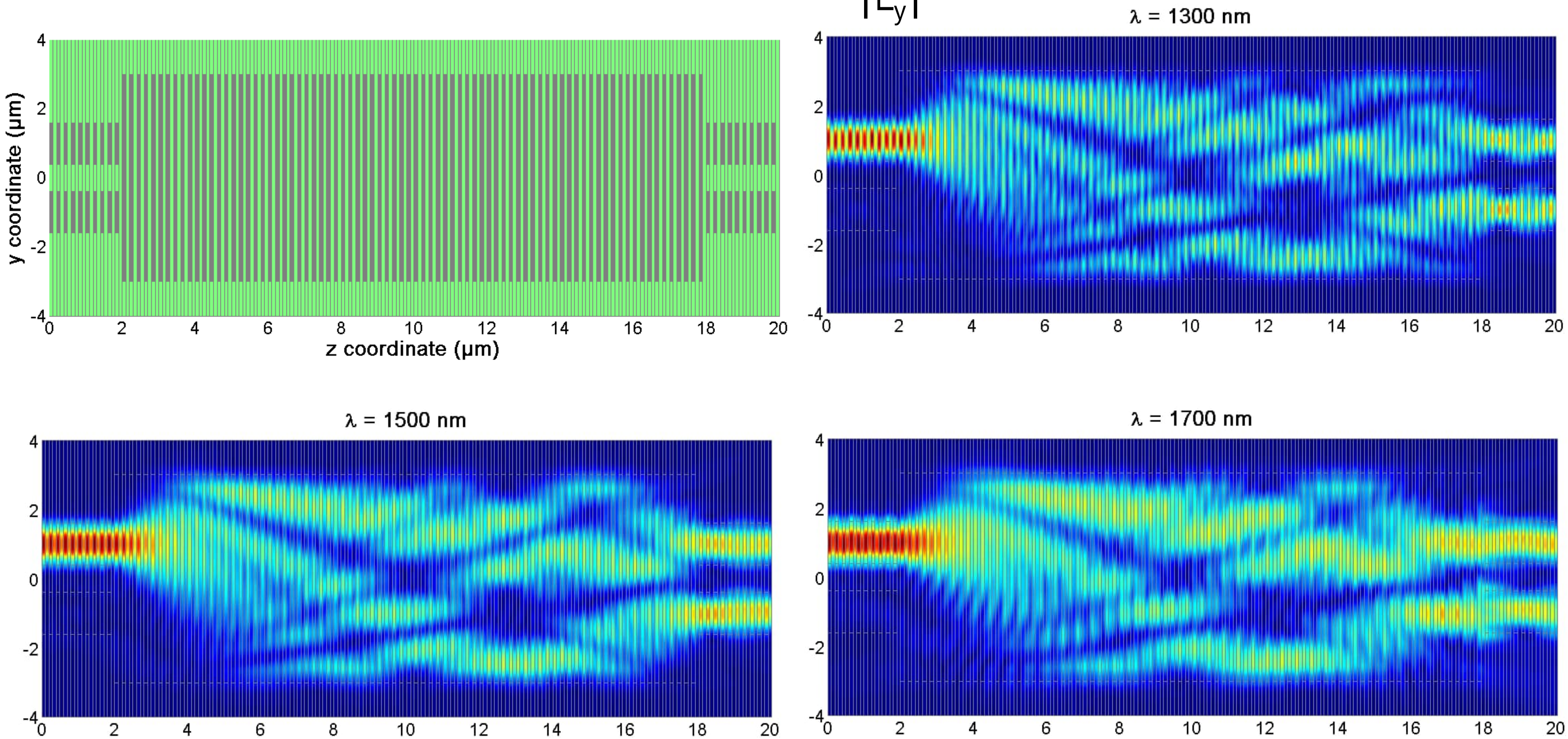

PROPERTIES OF INPUT AND OUTPUT COUPLERS

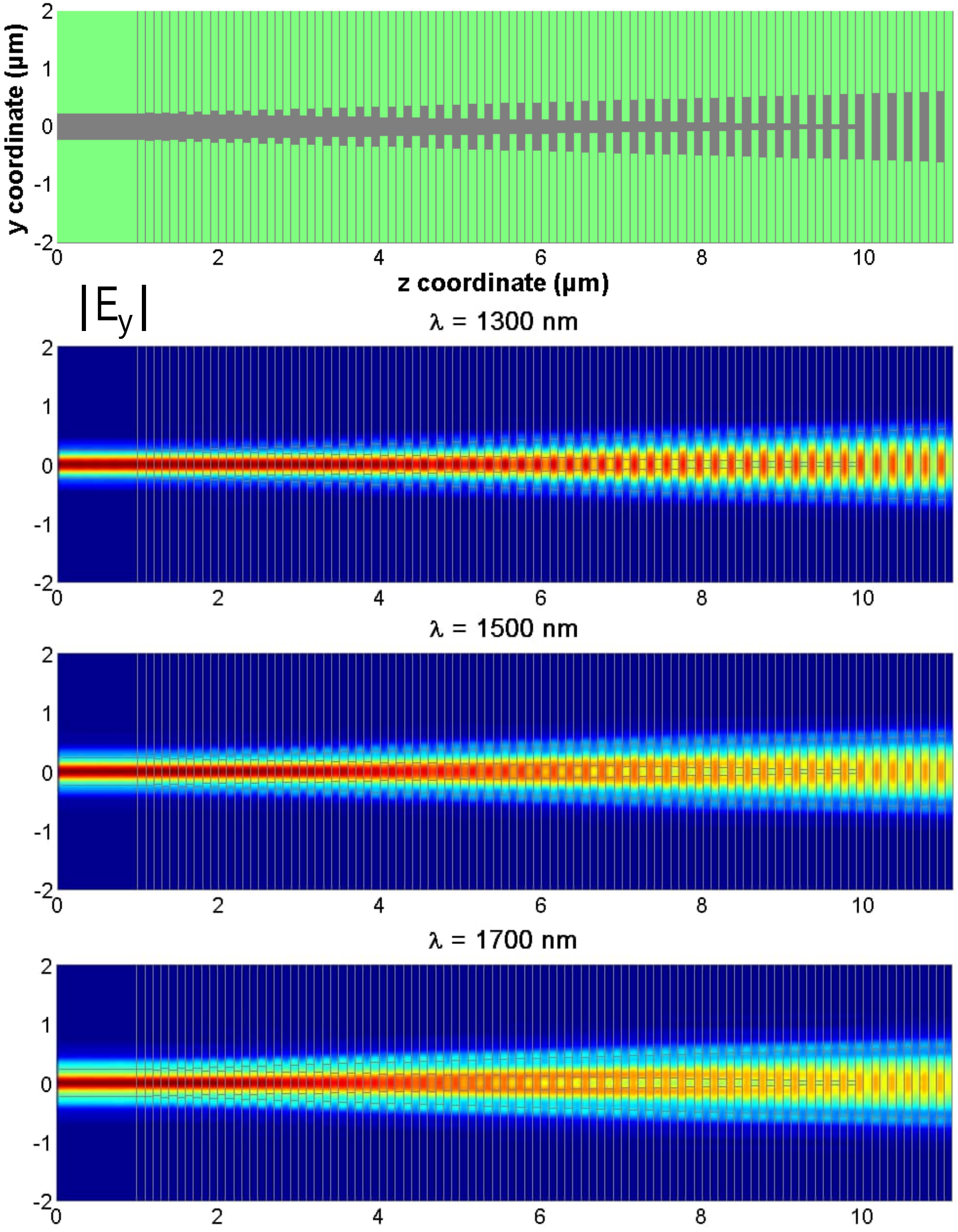

Estimated SWG period Λ = 200 nm

Conversion from photonic wire into Bloch mode of the SWG output:

Very high conversion efficiency difficult to reliably calculate (loss <= 0.01 dB), very small return loss – reflected power <= – 45 dB for all wavelengths 1.3 μm, 1.5 μm, and 1.7 μm.

Shorter taper could probably work well, too.

CHECK OF MUTUAL COUPLING IN THE TAPERS

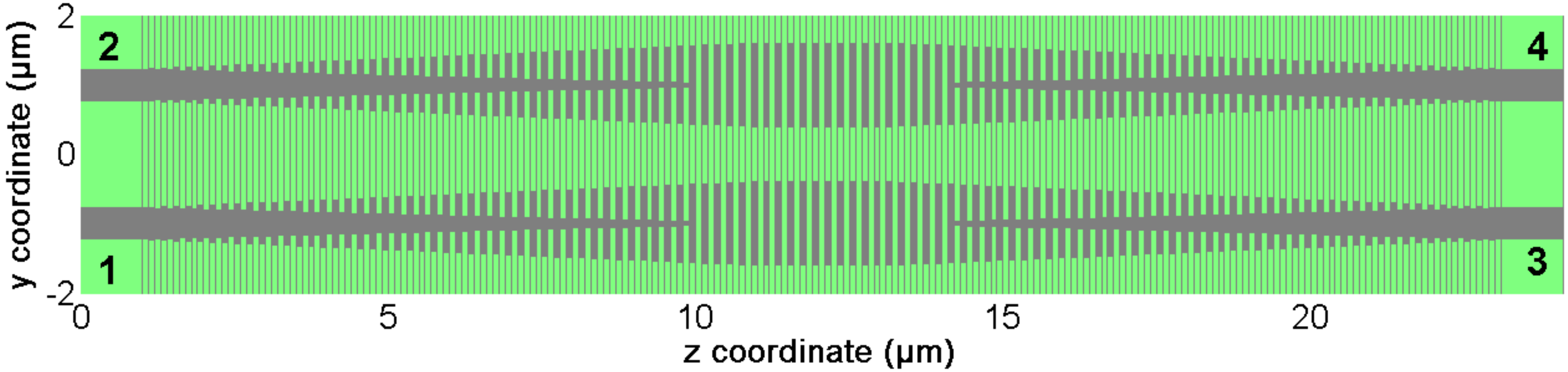

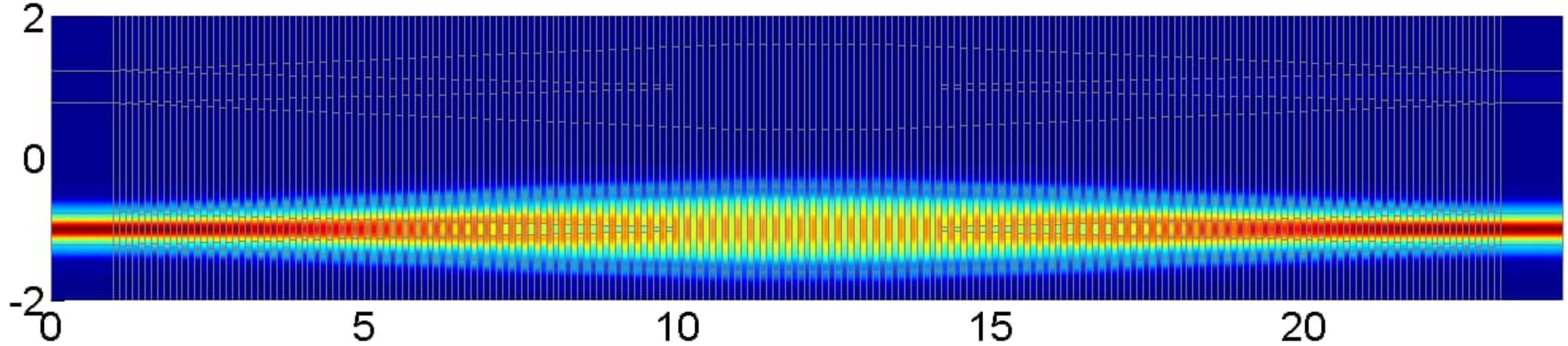

Calculated scattering parameters:

λ (μm)	$\lvert S_{11}\rvert^2$	$\lvert S_{31}\rvert^2$	$\lvert S_{41}\rvert^2$	Loss
1.70	2.304×10^{-5}	0.995	4.963×10^{-3}	-1.561×10^{-5}
1.50	2.804×10^{-5}	0.993	6.991×10^{-3}	-2.611×10^{-4}
1.30	4.149×10^{-5}	0.988	1.260×10^{-2}	-3.966×10^{-4}

Mutual coupling in tapers is unimportant

FIELD DISTRIBUTION IN THE SWG MMI COUPLER

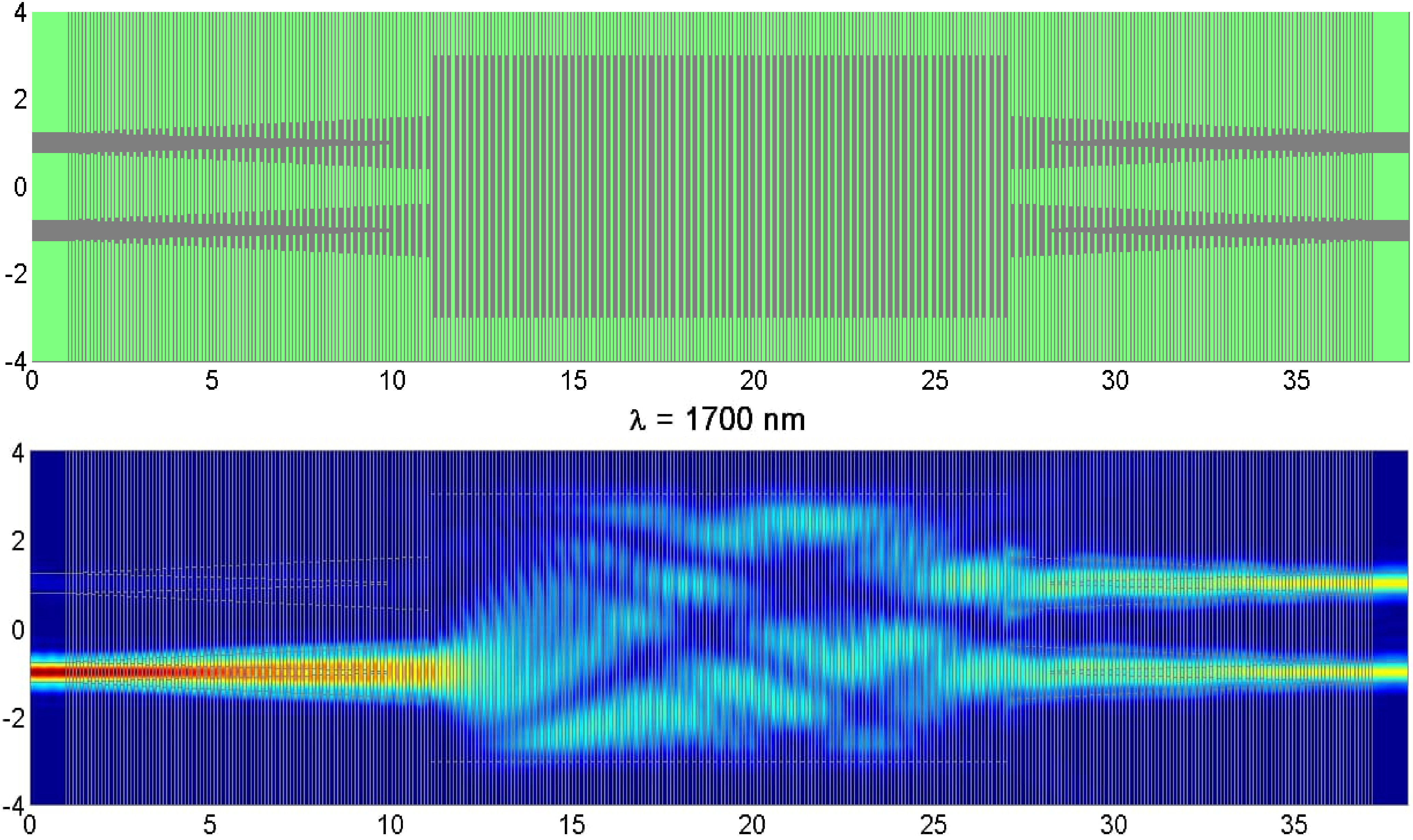

S-PARAMETERS OF THE COMPLETE MMI DEVICE

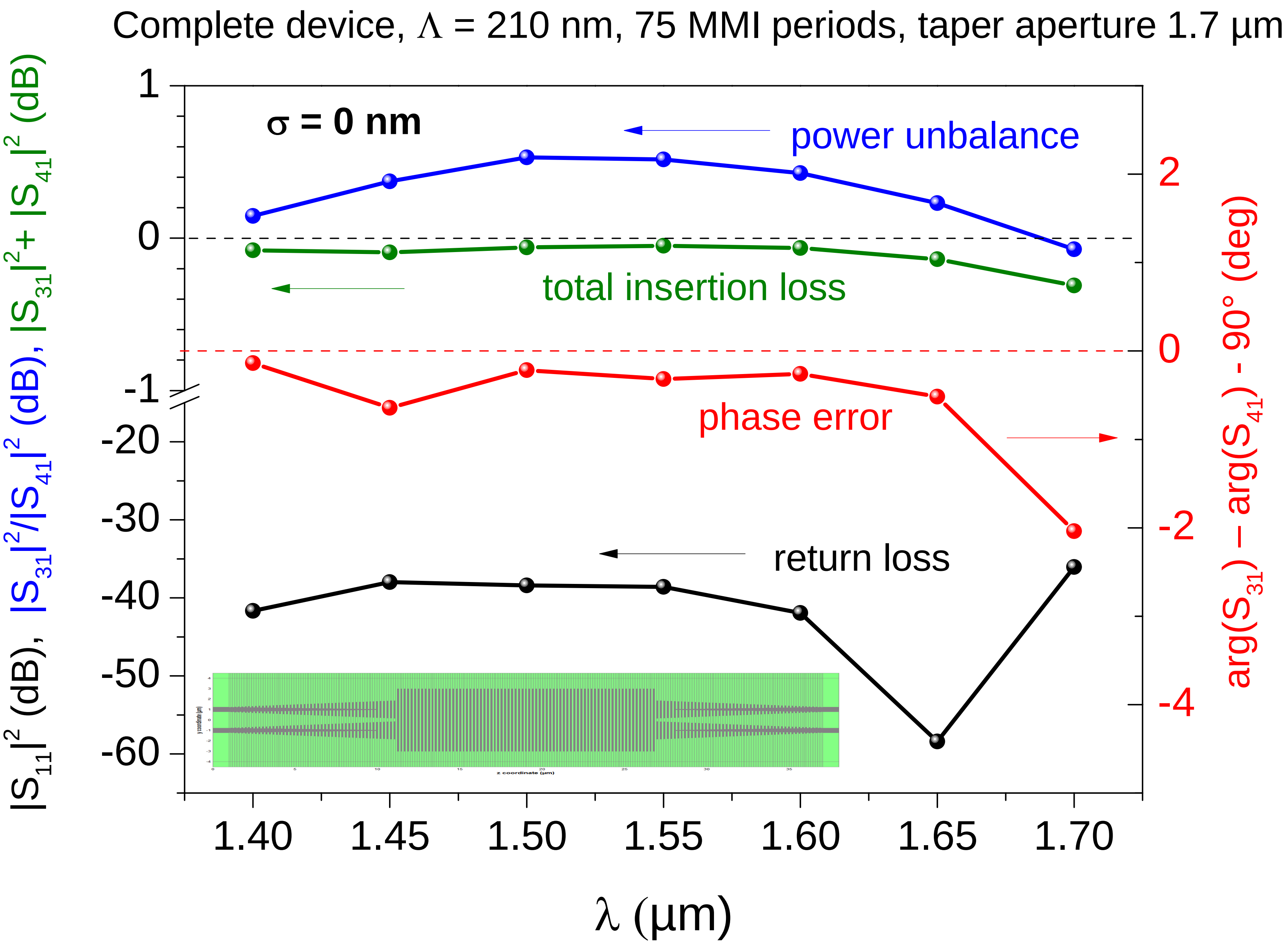

INFLUENCE OF RANDOM FLUCTUATIONS

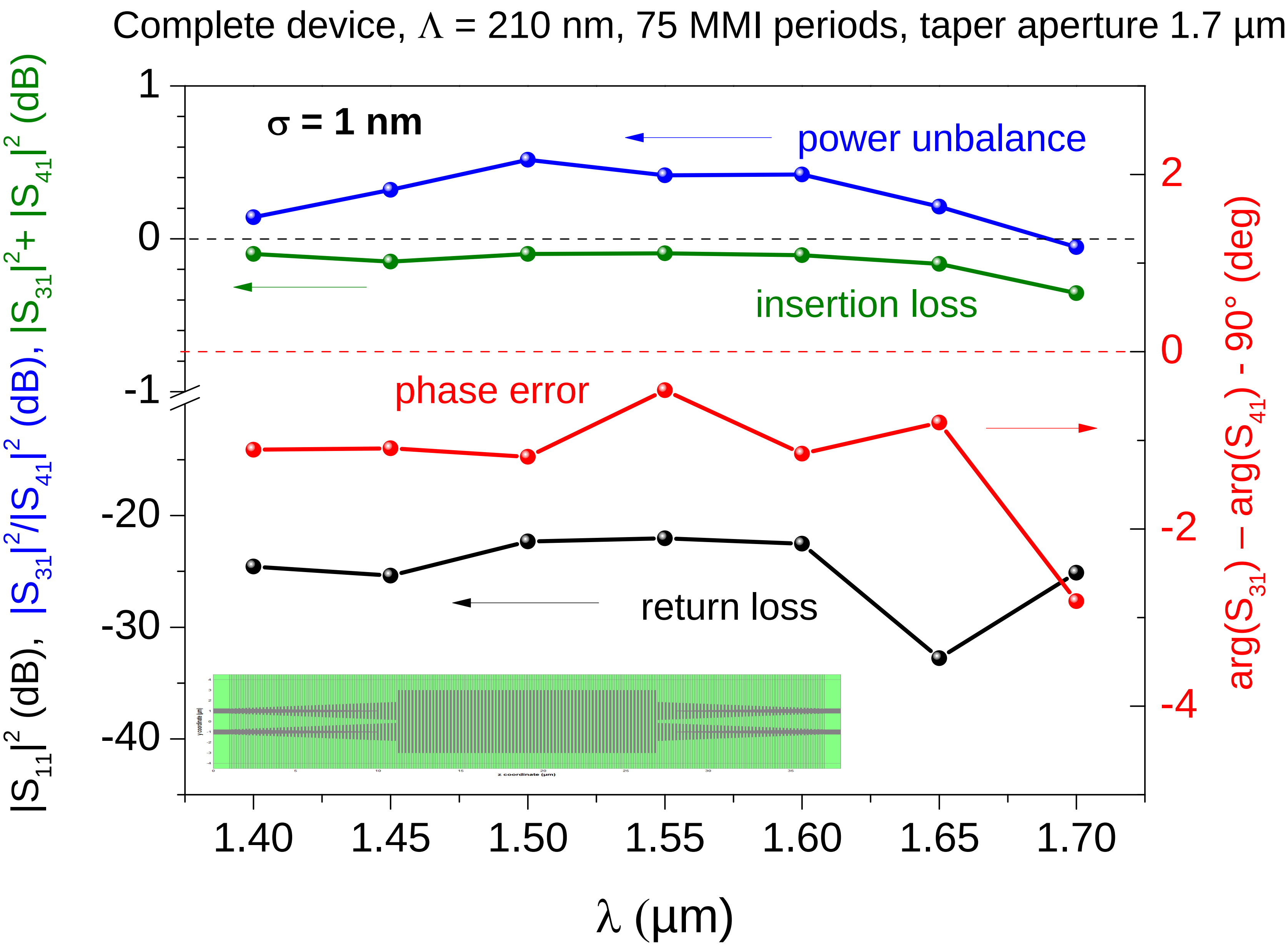

INFLUENCE OF RANDOM FLUCTUATIONS

Complete device, Λ = 210 nm, 75 MMI periods, taper aperture 1.7 μm

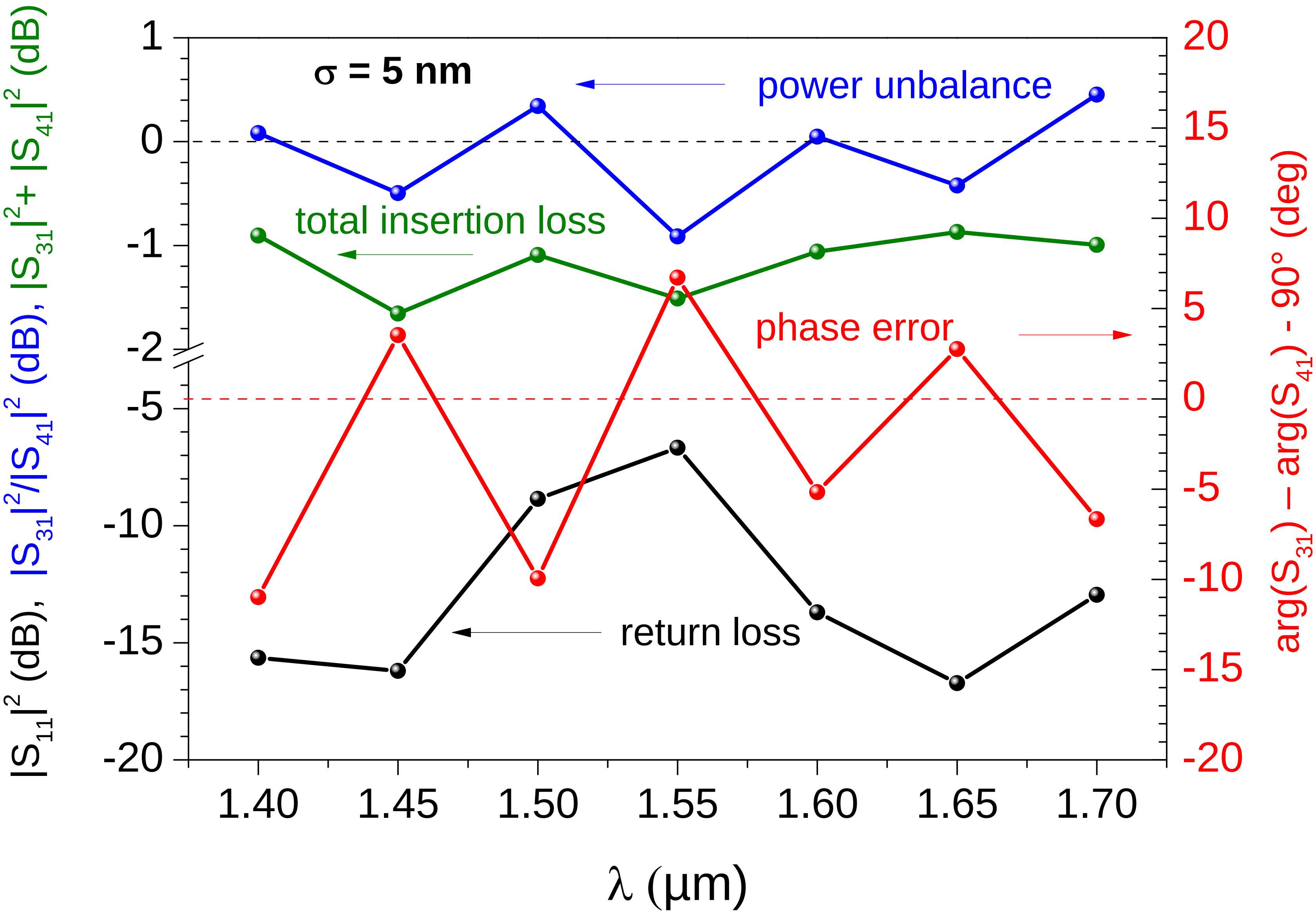

Bragg gratings in conventional SOI waveguides

Surface modulation

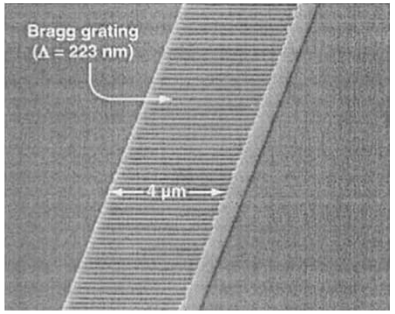

T. E. Murphy et al.,
JLT 19, 1938-1942 (2001).

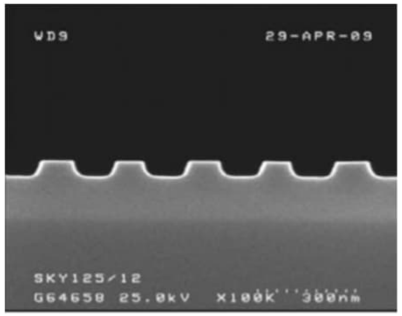

I. Giuntoni et al.,
IEEE PTL 21, 1894-1896 (2009).

Side modulation

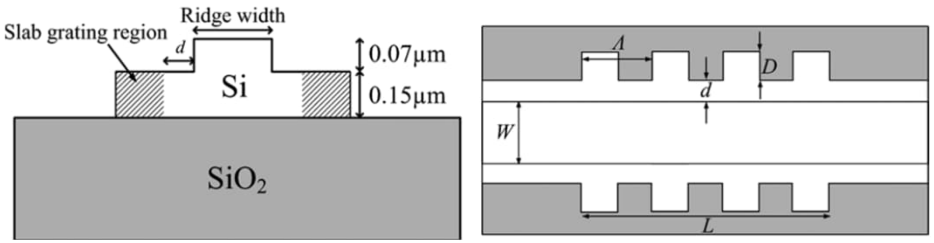

G. M. Jiang et al.,*IEEE PTL* 23, 6-8 (2011).

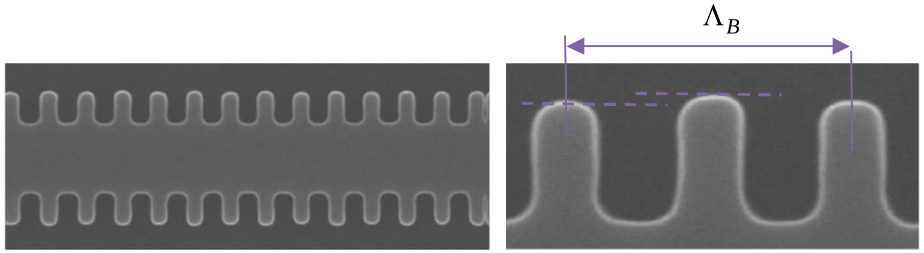

D. Pérez-Galacho et al., *Opt. Lett.* 42, 1468-1471 (2017).

Loading segments

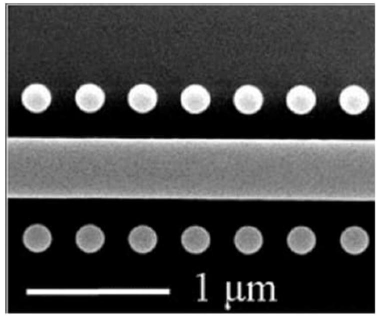

S. Zamek et al.,
Opt. Lett. 35, 3477-3479 (2010).

Tuning of coupling strength

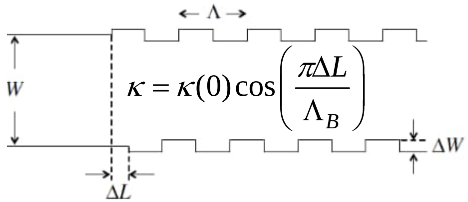

X. Wang et al.
Opt. Lett. 39, 5519-5522 (2014).

P. Cheben, J. Čtyroký et al., "Bragg filter bandwidth engineering in subwavelength grating metamaterial waveguides," Opt. Lett., vol. 44, no. 5, p. 1043, 2019

SWG COUPLERS FOR SOI PLATFORM

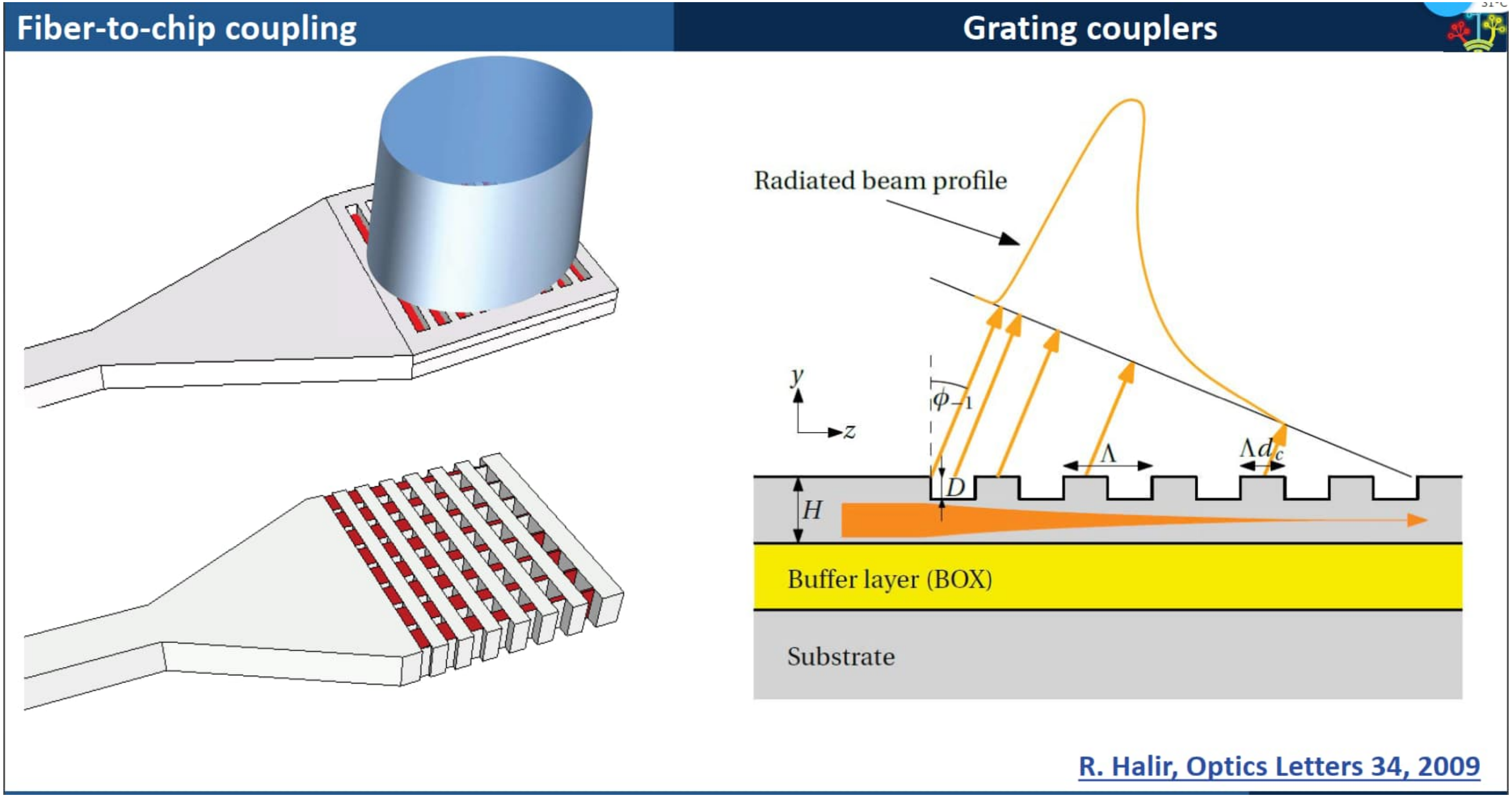

SWG COUPLERS FOR SOI PLATFORM

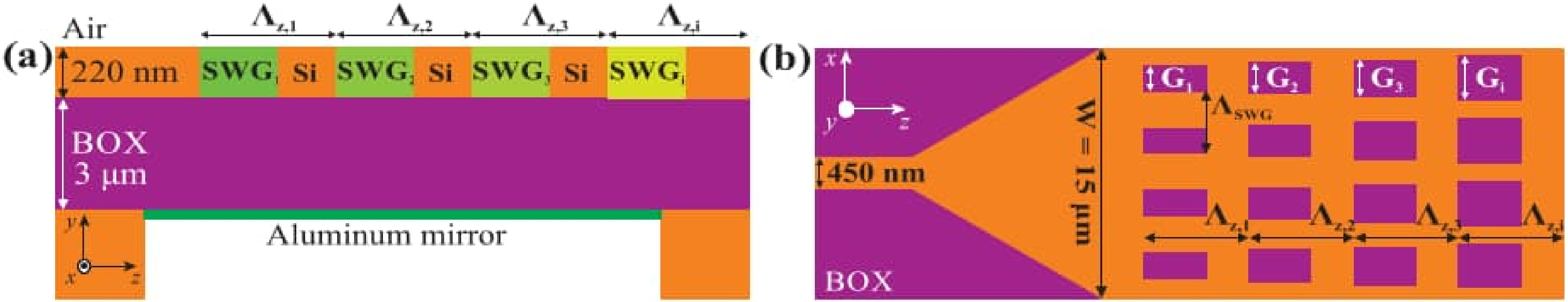

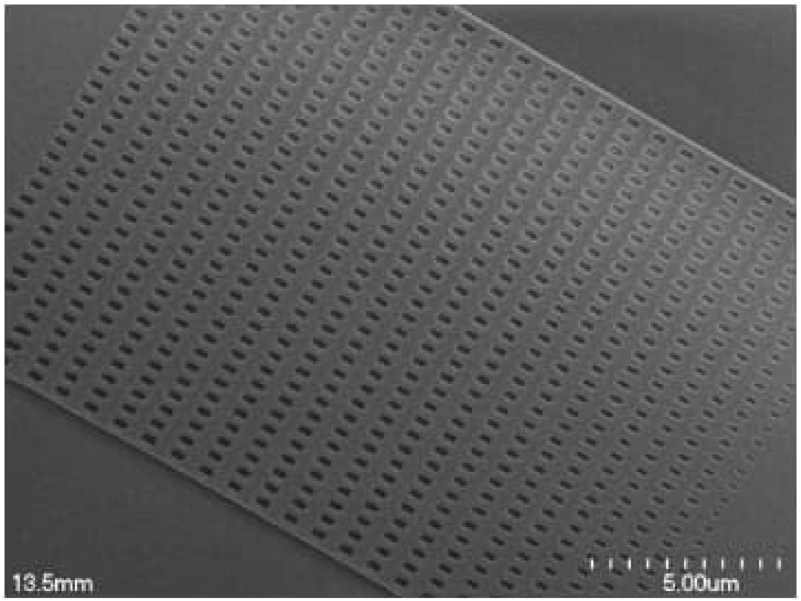

D. Benedikovic, P. Cheben, J. H. Schmid, D.-X. Xu, B. Lamontagne, S. Wang, J. Lapointe, R. Halir, A. Ortega-Moñux, S. Janz, and M. Dado, Opt. Express 23(17), 22628-22635 (2015).

TILTED SUBWAVELENGTH GRATING WAVEGUIDES

J. M. Luque-Gonzalez, A. Herrero-Bermello, A. Ortega-Monux, I. Molina-Fernandez, A. V. Velasco, P. Cheben, J. H. Schmid, S. Wang, and R. Halir, Opt. Lett. 43(19), 4691-4694 (2018).

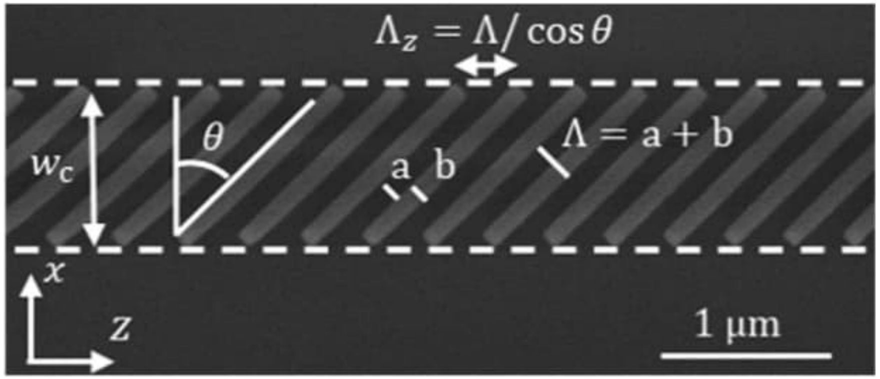

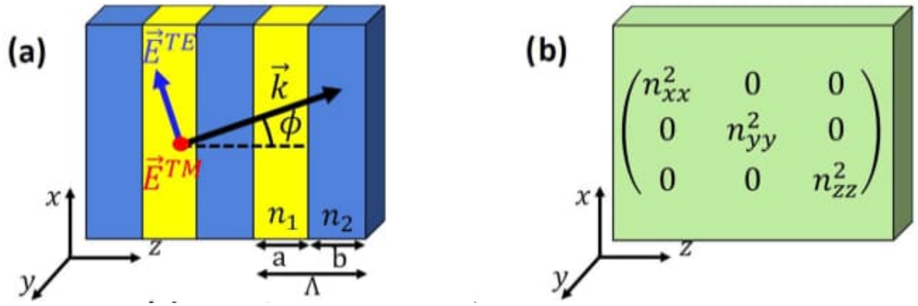

$$\tilde{\varepsilon}_{xx} = n_{xx}^2 \cos^2(\theta) + n_{zz}^2 \sin^2(\theta),$$

$$\tilde{\varepsilon}_{yy} = n_{yy}^2,$$

$$\tilde{\varepsilon}_{zz} = n_{xx}^2 \sin^2(\theta) + n_{zz}^2 \cos^2(\theta),$$

$$\tilde{\varepsilon}_{xz} = (n_{zz}^2 - n_{xx}^2) \cos(\theta) \sin(\theta).$$

Tilted planar SWG waveguide can be considered as an artificial *biaxially anisotropic medium*

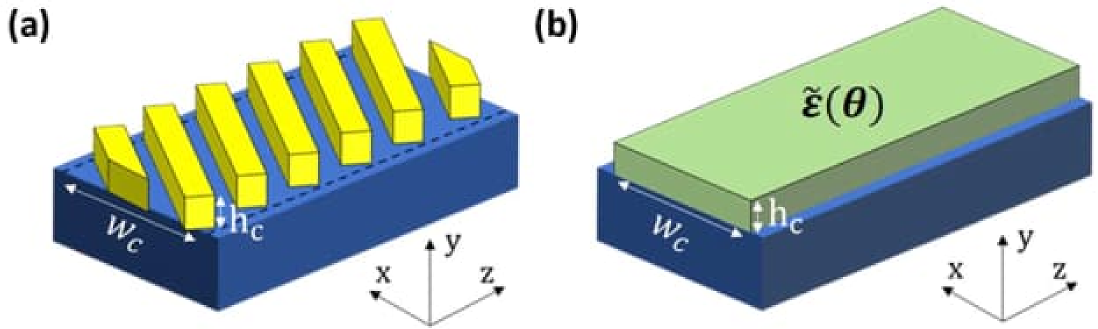

TILTED SUBWAVELENGTH GRATING WAVEGUIDES

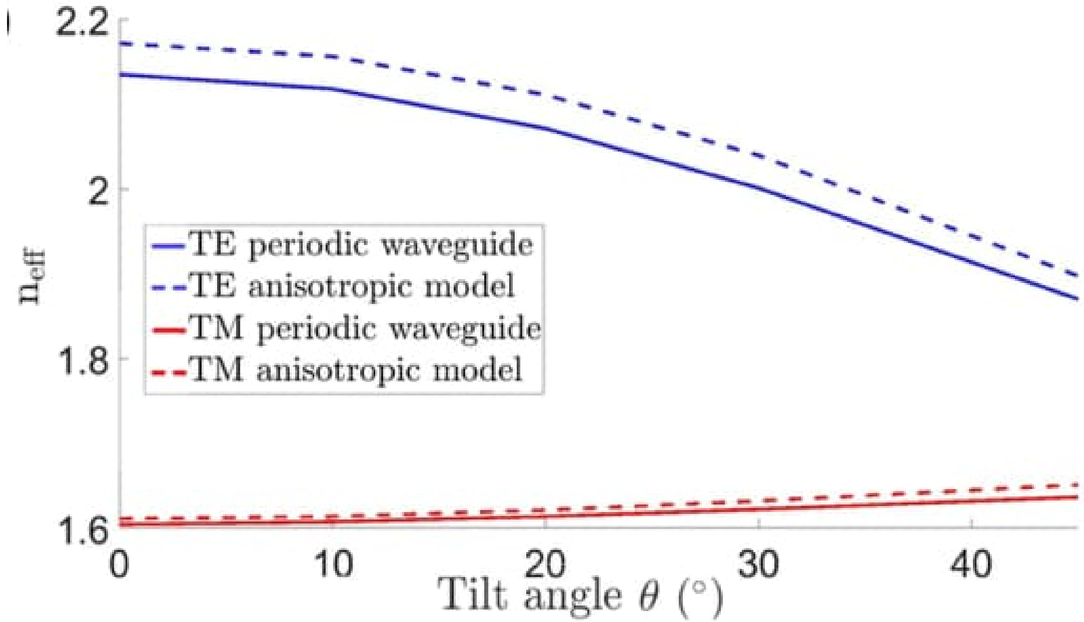

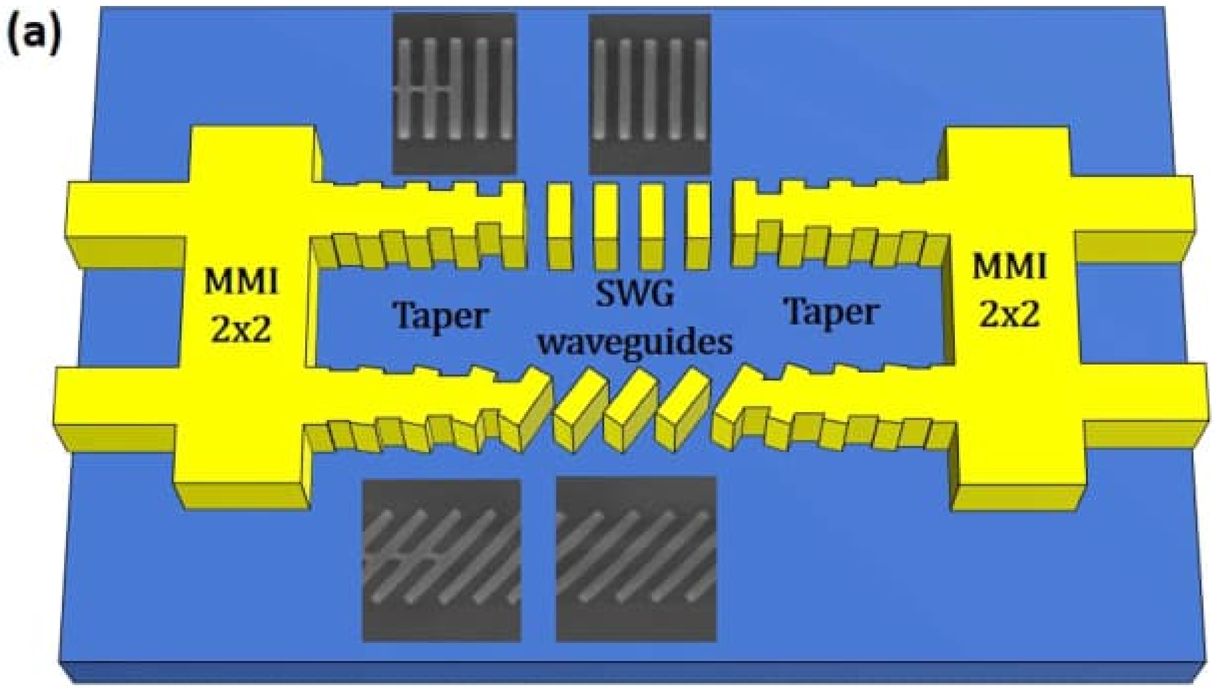

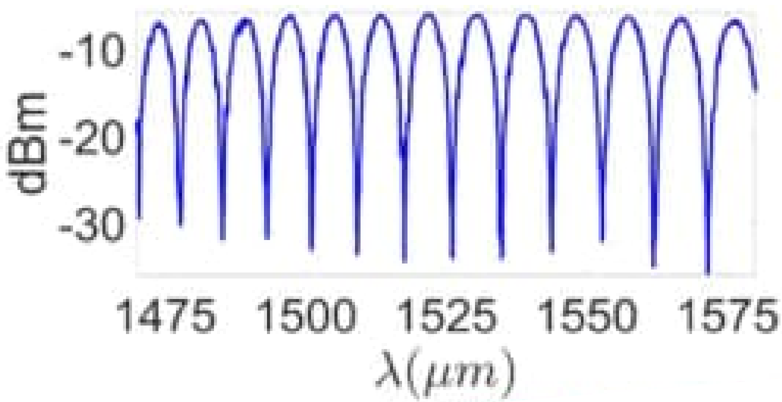

TILTED SWG WAVEGUIDE POLARIZATION SPLITTER

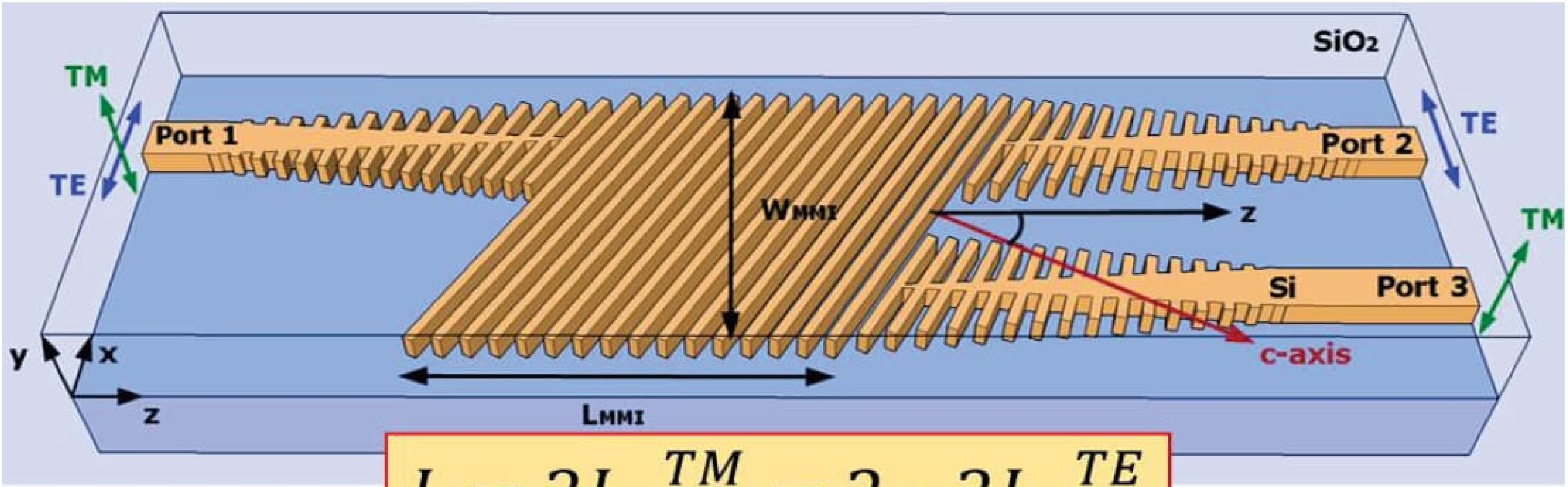

$$L = 3L_{\pi}^{TM} = 2 \cdot 3L_{\pi}^{TE}$$

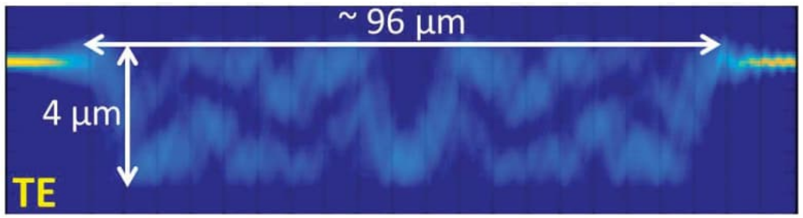

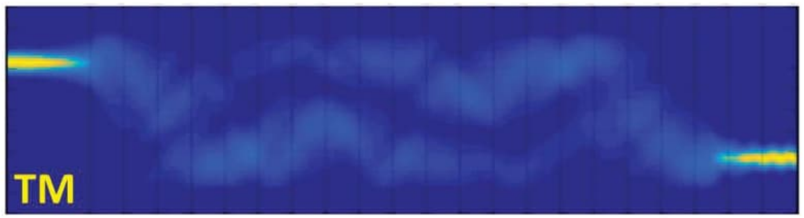

A. Herrero, Optics Letters, 2020

Uniform and apodized SWG Bragg gratings with loading segments

Uniform

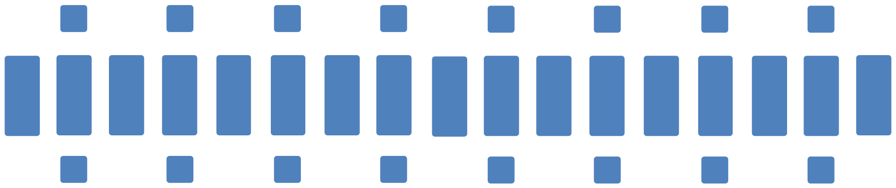

Apodized by symmetric shift

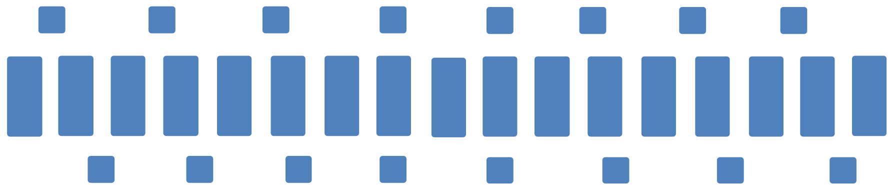

Apodized by separation

Apodized by symmetric shift with phase step

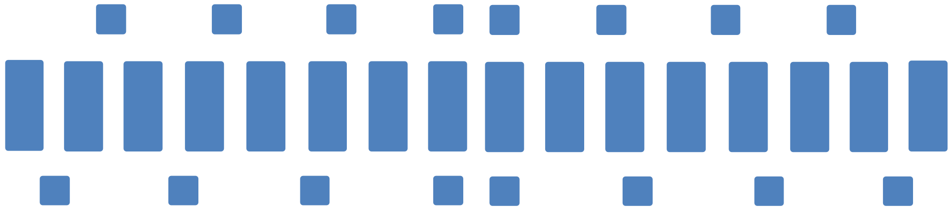

Apodized by asymmetric shift

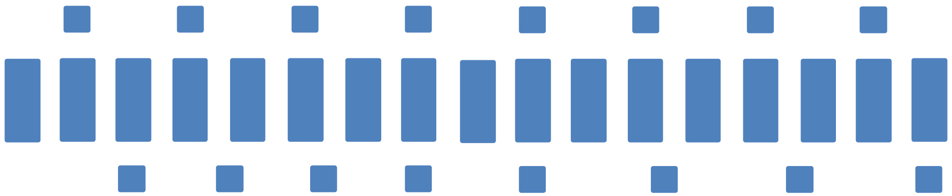

Design of such aperiodic structures using full-wave 3D methods (e.g., FMM) is impractical -> Coupled Mode Theory

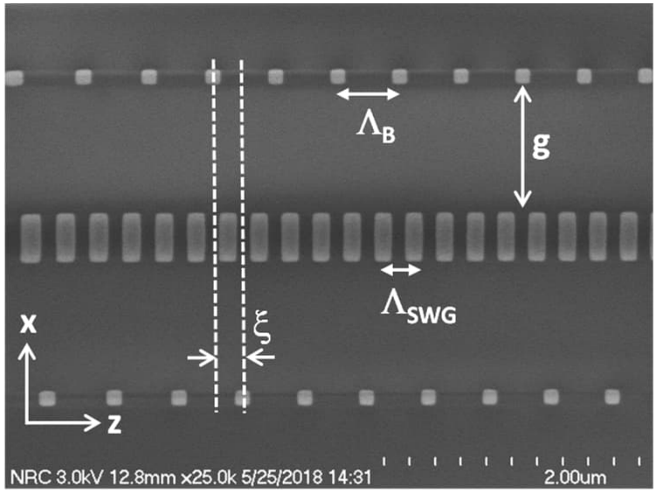

Λ$_B$
g
Λ$_{SWG}$
ξ
x
z
NRC 3.0kV 12.8mm x25.0k 5/25/2018 14:31
2.00um

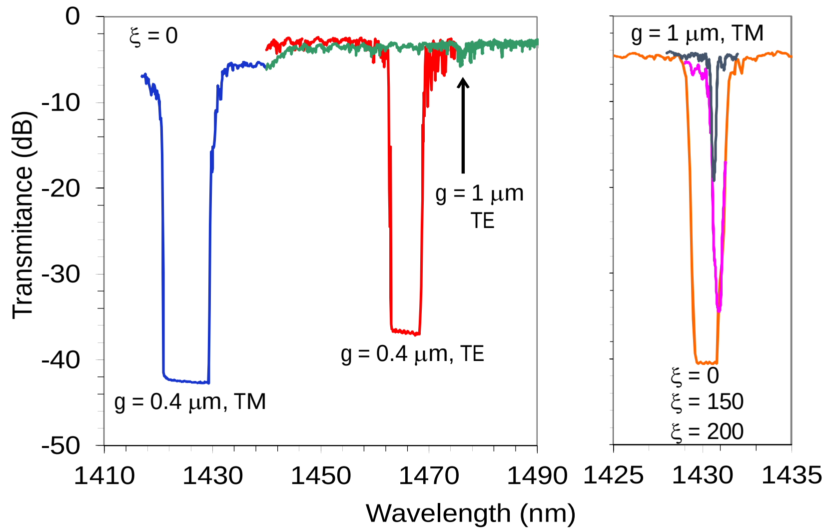

ξ = 0
g = 1 μm TE
g = 0.4 μm, TE
g = 0.4 μm, TM
g = 1 μm, TM
ξ = 0
ξ = 150
ξ = 200
Transmitance (dB)
0
-10
-20
-30
-40
-50
1410
1430
1450
1470
1490
1425
1430
1435
Wavelength (nm)

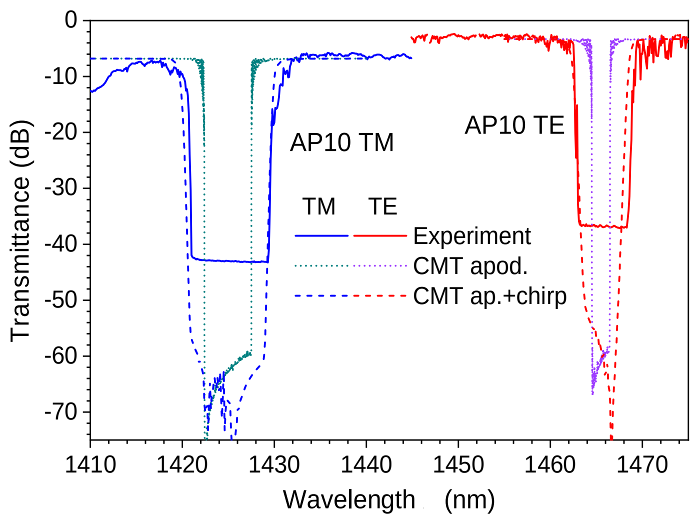

AP10 TM
AP10 TE
TM
TE
Experiment
CMT apod.
CMT ap.+chirp
Transmittance (dB)
0
-10
-20
-30
-40
-50
-60
-70
1410
1420
1430
1440
1450
1460
1470
Wavelength (nm)

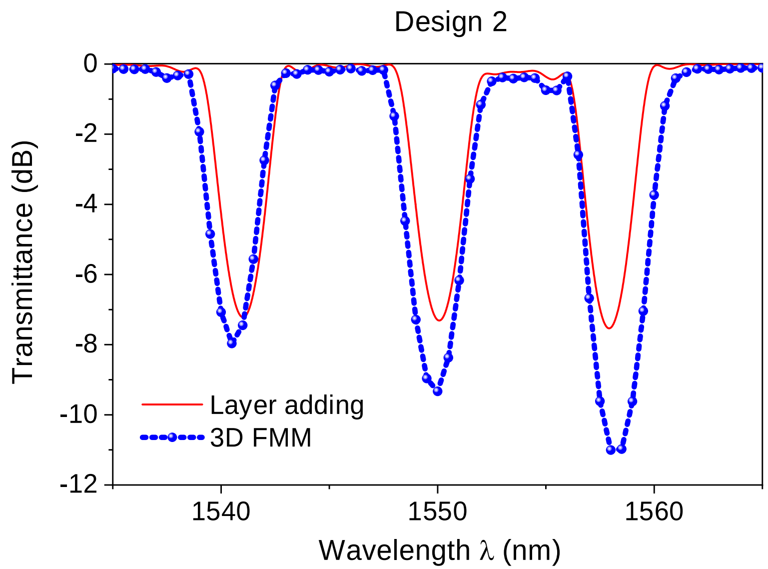

Design 2
Layer adding
3D FMM
Transmittance (dB)
0
-2
-4
-6
-8
-10
-12
1540
1550
1560
Wavelength λ (nm)

Bragg filter design – Daniel Pereira (Uni Malaga, internship at ÚFE, 15 Sept. – 15 Dec. 2019)

Filters with sinusoidal apodization of ***κ*** (suppression of sidelobes)

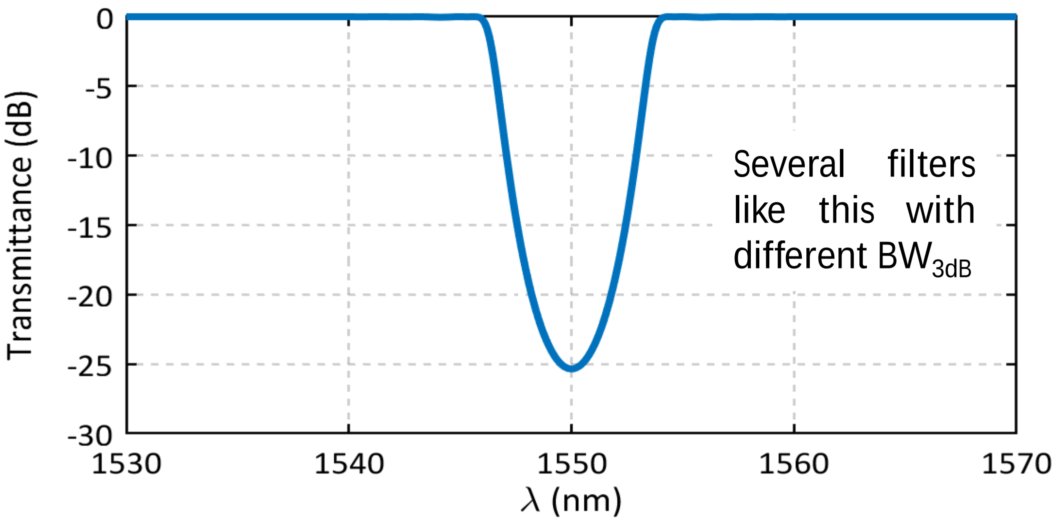

Square flat-top filters (multiple DWDM channels)

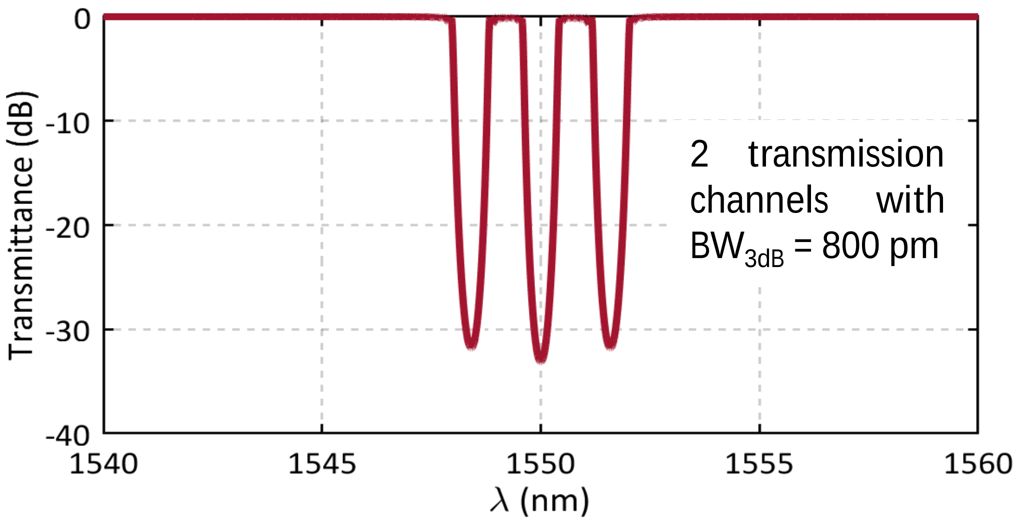

Atmospheric filtering (20 notches of $BW_{3dB} \approx$ 400 pm)

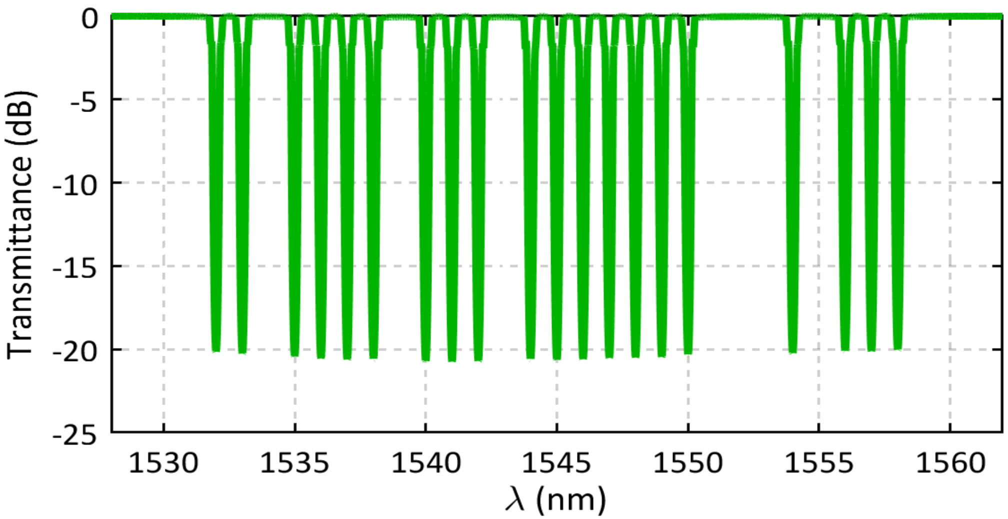

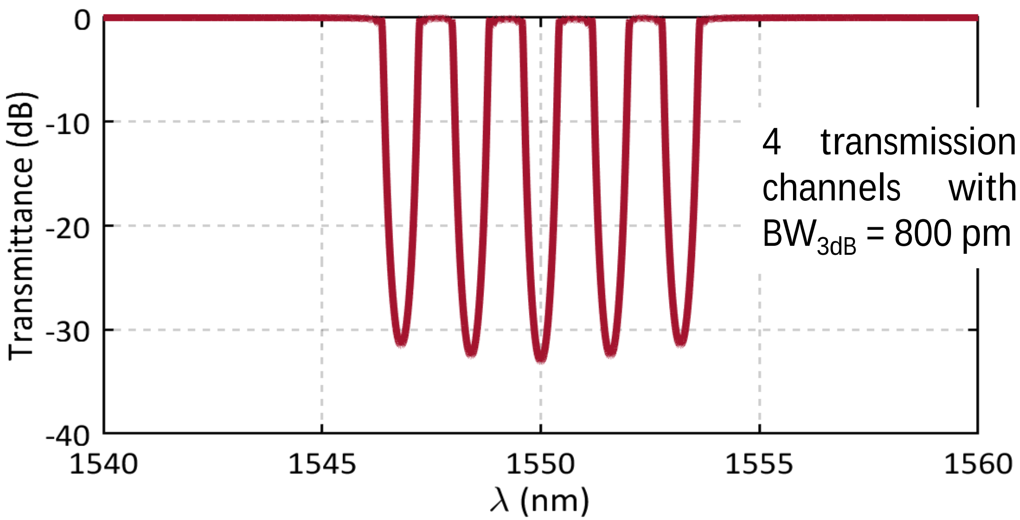

Preparation of mask for fabrication

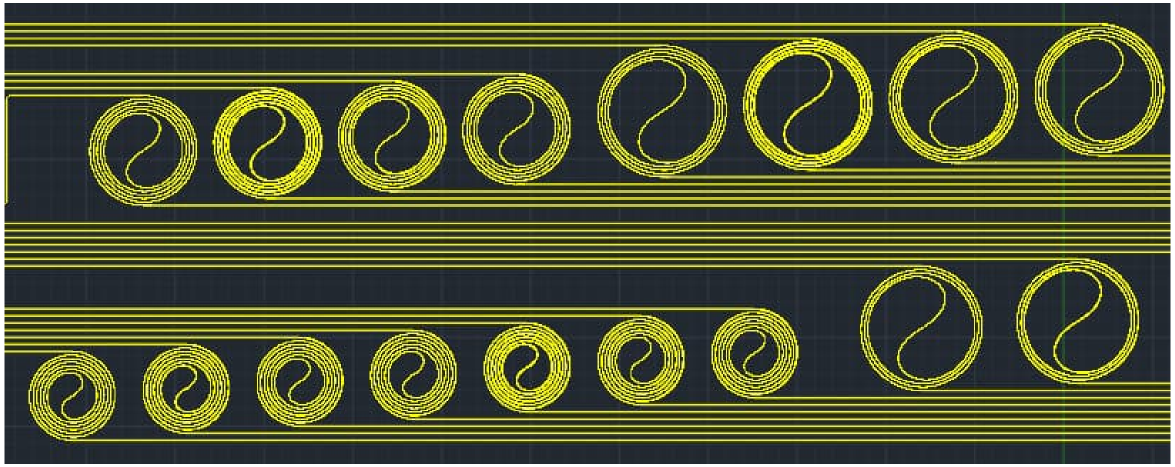

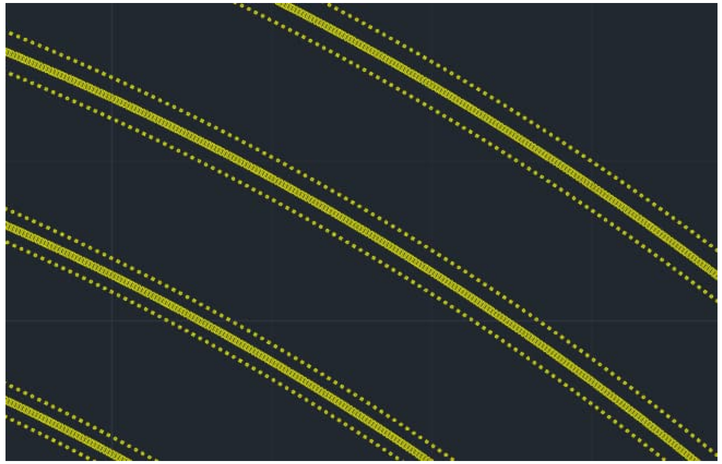

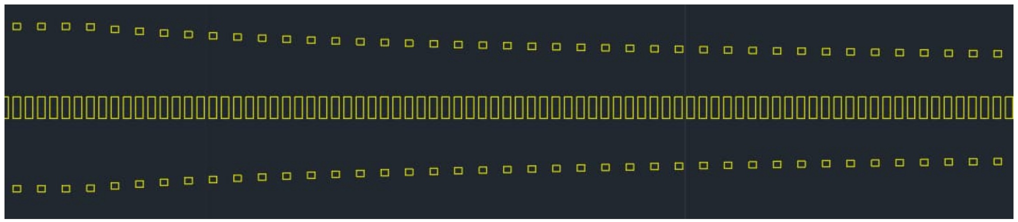

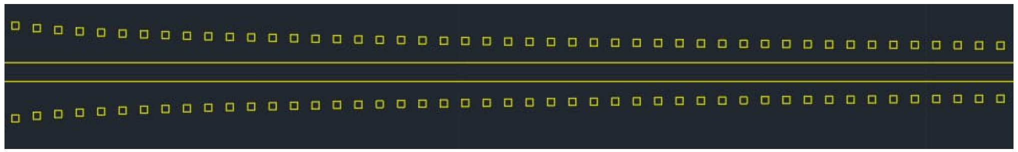

First experimental results of apodized Bragg filters will be obtained during next year

Designing High Performance Devices in Silicon Using Subwavelength Structures

Prof. Robert Halir

University of Malaga (Spain)
Andalusian Institute for Nano-medicine and Biotechnology (Bionand)

*You can find more information about subwavelength integrated photonics on the **review** co-authored by Dr. Halir and recently published by **Nature**: P. Cheben, et al. "Subwavelength integrated photonics." Nature 560.7720 (2018)*

OSA Optoelectronics Technical Group